



Research article

An improved finite difference and Galerkin spectral method for the fourth-order time fractional partial differential equations

Hanmei Jian, Junying Cao and Ziqiang Wang*

School of Data Science and Information Engineering, Guizhou Minzu University, Guiyang 550025, China

* **Correspondence:** Email: wzq@gzmu.edu.cn.

Abstract: We investigated a numerical scheme for the fourth-order time fractional partial differential equations by employing the temporal $L2$ scheme and spatial Legendre-Galerkin spectral method. The stability and error estimation of the present scheme were proved by combining partial integration, the properties of the inverse Laplace operator with respect to initial values, and the right-hand function. The error estimation indicated that the present scheme has spectral accuracy convergence in space and $(3 - \kappa)$, $\kappa \in (0, 1)$, uniform accuracy in time. Three numerical examples verified the theoretical convergence order in time and space.

Keywords: fourth-order partial differential equation; high-order temporal accuracy; Legendre-Galerkin method; error estimation; stability analysis

Mathematics Subject Classification: 65L12, 65M06, 65M12

1. Introduction

Fourth-order partial differential equations with time-fractional derivative have been widely applied in various fields, because they can describe many complex physical engineering and life phenomena more accurately. This includes applications in environmental science, high-energy physics, fluid dynamics, electronic science, diffusion, heat transfer, solid mechanics, bridge slabs, floor systems, window glass, airplane wings, and the problems of non-stationary and nonlinear systems such as economic and biological systems [1, 2]. Therefore, constructing a high-order numerical solution of a fourth-order partial differential equation is a significant research topic. This paper will consider the temporal high-order uniform accuracy numerical for the fourth-order time fractional partial differential equation (TFPDE). Many numerical schemes have been developed to solve fourth-order TFPDEs, such as the quintic spline technique [3], Legendre-Galerkin spectral method [4], mixed finite element method [5], radial basis functions [6], mixed Legendre-Galerkin approximations [7], compact

difference scheme [8, 9], and B-spline collocation method [10], etc.

We consider the following equations:

$$\begin{cases} {}_0D_t^\kappa z(\mathbf{x}, t) + \Delta^2 z(\mathbf{x}, t) = f(\mathbf{x}, t), & (\mathbf{x}, t) \in \Omega \times I, \\ z(\mathbf{x}, t) = \frac{\partial z(\mathbf{x}, t)}{\partial n} = 0, & (\mathbf{x}, t) \in \partial\Omega \times I, \\ z(\mathbf{x}, 0) = z_0(\mathbf{x}), & \mathbf{x} \in \Omega, \end{cases} \quad (1.1)$$

$$\begin{cases} {}_0D_t^\kappa z(\mathbf{x}, t) + \Delta^2 z(\mathbf{x}, t) = f(\mathbf{x}, t), & (\mathbf{x}, t) \in \Omega \times I, \\ z(\mathbf{x}, t) = \frac{\partial z(\mathbf{x}, t)}{\partial n} = 0, & (\mathbf{x}, t) \in \partial\Omega \times I, \\ z(\mathbf{x}, 0) = z_0(\mathbf{x}), & \mathbf{x} \in \Omega, \end{cases} \quad (1.2)$$

$$\begin{cases} {}_0D_t^\kappa z(\mathbf{x}, t) + \Delta^2 z(\mathbf{x}, t) = f(\mathbf{x}, t), & (\mathbf{x}, t) \in \Omega \times I, \\ z(\mathbf{x}, t) = \frac{\partial z(\mathbf{x}, t)}{\partial n} = 0, & (\mathbf{x}, t) \in \partial\Omega \times I, \\ z(\mathbf{x}, 0) = z_0(\mathbf{x}), & \mathbf{x} \in \Omega, \end{cases} \quad (1.3)$$

where the bounded area of the Lipschitz continuous boundary $\partial\Omega$ is $\Omega = \prod_{i=1}^d (a_i, b_i)$ with $d \geq 1$ as the dimension of the space. $\mathbf{x} = (x_1, x_2, \dots, x_d) \in \mathbb{R}^d$, Δ is a Laplace operator, Δ^2 means applying the Laplacian twice, $T > 0$, $0 < \kappa < 1$, and $I = (0, T]$, κ is the order of the temporal fractional derivative, n is the outward normal unit vector, and the function $f(\mathbf{x}, t) \in \Omega \times I$. In (1.1), ${}_0D_t^\kappa z$ is the κ -order Caputo fractional derivative, defined as:

$${}_0D_t^\kappa z(\mathbf{x}, t) = \frac{1}{\Gamma(1-\kappa)} \int_0^t \frac{\partial_\tau z(\mathbf{x}, \tau)}{(t-\tau)^\kappa} d\tau, \quad 0 < \kappa < 1,$$

where $\Gamma(\cdot)$ represents the gamma function. The minimum condition for the existence of the Caputo derivative ${}_0D_t^\kappa z(\mathbf{x}, t)$ of order between 0 and 1 of a function is that the function is absolutely continuous on the interval of interest.

The research on the high-order efficient numerical scheme for fourth-order TFPDEs has always been one of the hot topics in TFPDEs, and many researchers have made significant research achievements in fourth-order TFPDEs. In [11], a space-time Petrov-Galerkin spectral method for the fourth-order TFPDE was explored. In [12], they gave a numerical scheme for the fourth-order TFPDE by the Petrov-Galerkin approach in time and the Galerkin approximation in space. In [13], they presented an $L2$ scheme and the fourth-order compact numerical differential method for solving fourth-order TFPDEs. In [14], a mixed virtual element method was used to solve fourth-order TFPDEs with an initial weak singularity solution. Based on the implicit method, an efficient numerical scheme was constructed for fourth-order TFPDEs in [15]. In [16], they used the graded $L1$ scheme and the local discontinuous Galerkin method to solve the TFPDE in time and space, respectively. In [17], they proposed a compact difference-Galerkin spectral method that can handle some complex boundary cases. In [18], they used the $L2$ scheme and direct meshless local Petrov-Galerkin technique to solved the fourth-order TFPDE in time and space with the convergence order and unconditional stability. In [19], a new method was presented and the shifted fractional Jacobi collocation method was extended to solve the fourth-order TFPDE. They proposed an effective Galerkin spectral method to solve the fourth-order TFPDE in complex regions in [20]. A spectral-Galerkin method for the fourth-order problem of cylindrical regions based on Legendre-Fourier approximation was studied in [21]. In [22], the spectral method for the fourth-order problem defined on a quadrilateral was studied. In [23], they used second-order finite differences and the Galerkin method for discretization to solve the fourth-order TFPDE with a weak singular kernel. In [24], they proposed a fully discrete scheme based on the shifted Grönwald difference scheme and local discontinuous Galerkin method, and studied the stability and convergence analysis. In [25], they introduced the quintic B-spline collocation method to solve fourth-order TFPDEs with high efficiency. In [26], a fast $(3 - \alpha)$ -order numerical method was proposed, which can be applied to

the TFPDE in bounded domains. In [27], the authors used the time-space spectral Galerkin method to solved fourth-order TFPDEs.

Considering that Galerkin spectral methods are an efficient numerical for the fourth-order partial differential equation, many researchers use the spectral method to solve fourth-order TFPDEs. Due to the exponential convergence of spectral methods, constructing a high-order temporal uniform accuracy numerical scheme is a very important research topic. The exiting high-order numerical schemes for the fourth-order TFPDE have the disadvantages of first-step theoretical convergence order reduction and the fact that the high-order numerical scheme is only for linear TFPDEs, being not theoretically suitable to solve the nonlinear case. In the spatial discretization, we use the Legendre-Galerkin spectral method for its ability to capture high spatial convergence accuracy with high computational efficiency. In the temporal discretization, we use an improved $L2$ scheme for its ability to obtain temporal high-order uniform accuracy. The stability of the fully discrete numerical scheme is strictly proved by using the inverse Laplace operator. The improved numerical scheme has the following contributions.

- An improved scheme for TFPDEs with spatial fourth-order is first established with uniform high-order accuracy in time.
- The stability and error estimation of the present scheme are strictly based on the properties of the inverse Laplace operator and the appropriate parameter transformations to transform the numerical scheme into an equivalent form, where all the coefficients are positive.
- The improved numerical scheme can be used to solve linear and non-linear fourth-order TFPDEs.

The structure of this article is as follows: In Section 2, we first describe the semi-discrete scheme of the time fractional derivative and present the truncation error, and then construct the fully discrete scheme of the fourth-order TFPDE. In Section 3, the stability and error estimation of the scheme are established. In Section 4, we give some numerical experiments to verify the effectiveness of our method. In Section 5, we provide some concluding remarks.

2. Full discretization numerical scheme for the fourth-order TFPDE

First, we present the high-order uniform accuracy temporal scheme for the time fractional derivative (1.1) by using the following $L2$ scheme. Let us assume $t_m = m\tau$, for $m = 0, 1, \dots, K$, where $\tau = \frac{T}{K}$ is the time step. According to [28], set $\kappa_0 = \Gamma(3 - \kappa)\tau^\kappa$, and we can obtain the effective scheme of ${}_0D_t^\kappa z(\mathbf{x}, t_m)$ as follows:

$${}_0D_t^\kappa z(\mathbf{x}, t_m) = \begin{cases} \kappa_0^{-1} (\bar{A}_1 z(\mathbf{x}, t_0) + \bar{B}_1 z(\mathbf{x}, t_1) + \bar{C}_1 z(\mathbf{x}, t_2)), & m = 1, \\ \kappa_0^{-1} (\bar{A}_2 z(\mathbf{x}, t_0) + \bar{B}_2 z(\mathbf{x}, t_1) + \bar{C}_2 z(\mathbf{x}, t_2)), & m = 2, \\ \kappa_0^{-1} \{ \bar{A}_m z(\mathbf{x}, t_0) + \bar{B}_m z(\mathbf{x}, t_1) + \bar{C}_m z(\mathbf{x}, t_2) \\ + \sum_{l=1}^{m-1} [A_l z(\mathbf{x}, t_{m-l-1}) + B_l z(\mathbf{x}, t_{m-l}) + C_l z(\mathbf{x}, t_{m-l+1})] \}, & m \geq 3, \end{cases} \quad (2.1)$$

where

$$\begin{aligned} \bar{A}_1 &= (3\kappa - 4)/2, \quad \bar{B}_1 = 2(1 - \kappa), \quad \bar{C}_1 = \kappa/2, \\ \bar{A}_2 &= (3\kappa - 2)/2^\kappa, \quad \bar{B}_2 = -4\kappa/2^\kappa, \quad \bar{C}_2 = (\kappa + 2)/2^\kappa, \end{aligned}$$

$$\begin{aligned}
\bar{A}_m &= (2-\kappa)(m-1)^{1-\kappa}/2 - 3(2-\kappa)m^{1-\kappa}/2 + m^{2-\kappa} - (m-1)^{2-\kappa}, \quad m \geq 3, \\
\bar{B}_m &= 2(m-1)^{2-\kappa} - 2m^{2-\kappa} + 2(2-\kappa)m^{1-\kappa}, \quad m \geq 3, \\
\bar{C}_m &= -(2-\kappa) \left[m^{1-\kappa} + (m-1)^{1-\kappa} \right] / 2 + m^{2-\kappa} - (m-1)^{2-\kappa}, \quad m \geq 3, \\
A_l &= l^{2-\kappa} - (2-\kappa) \left[(l-1)^{1-\kappa} + l^{1-\kappa} \right] / 2 - (l-1)^{2-\kappa}, \\
B_l &= 2 \left[(2-\kappa)(l-1)^{1-\kappa} + (l-1)^{2-\kappa} - l^{2-\kappa} \right], \\
C_l &= (2-\kappa)l^{1-\kappa}/2 + l^{2-\kappa} - 3(2-\kappa)(l-1)^{1-\kappa}/2 - (l-1)^{2-\kappa}.
\end{aligned}$$

We will introduce the local truncation error estimate related to the proposed numerical discretization scheme (2.1) as the following Lemma 2.1.

Lemma 2.1. [28] Suppose that $z(\cdot, t)$ has a fourth derivative with respect to t :

$$|R_\tau^m| = \left| {}_0D_t^\kappa z(\cdot, t_m) - {}_0D_\tau^\kappa z(\cdot, t_m) \right| \leq C\tau^{3-\kappa}, \quad \forall m \geq 1, 0 < \kappa < 1, \quad (2.2)$$

where $C > 0$ is a constant independent of τ .

Second, we study the Galerkin spectral approximation of (1.1) in space. To simplify the notations, we let $\Omega = \prod_{i=1}^d (-1, 1)$ hereafter. Set

$$(u, w) = \int_{\Omega} u w d\Omega, \quad \forall u, w \in L^2(\Omega), \quad \|u\|_0^2 = (u, u), \quad \forall u \in L^2(\Omega),$$

and

$$Y = \left\{ v \in H^2(\Omega) : v|_{\partial\Omega} = \frac{\partial v}{\partial n}|_{\partial\Omega} = 0 \right\}, \quad (\Delta y, \Delta v) = \int_{\Omega} \Delta y \Delta v d\Omega, \quad \forall y, v \in Y.$$

Let

$$X_N^i = \text{span} \{L_0(x_i), L_1(x_i), \dots, L_N(x_i)\},$$

where $L_n(x_i)$ are n th Legendre polynomial for $i = 1, 2, \dots, d$. We now define a product space, described as follows:

$$X_N = \prod_{i=1}^d X_N^i.$$

We denote by Q_N the space consisting of all algebraic polynomials of each degree less than or equal to N . We introduce the following finite-dimensional space $Y_N = X_N \cap Y$, i.e.,

$$Y_N := \left\{ v_N \in Q_N : v_N|_{\partial\Omega} = \frac{\partial v_N}{\partial n}|_{\partial\Omega} = 0 \right\}.$$

In order to analysis the convergence and stability of the full discrete scheme, we define the norm $\|\cdot\|_2$ as follows:

$$\|\cdot\|_2 = \left(\|\cdot\|_0^2 + \kappa_0 \beta_0^{-1} \|\Delta \cdot\|_0^2 \right)^{\frac{1}{2}}, \quad (2.3)$$

where $\beta_0 = \frac{4-\kappa}{2} > 0, \forall \kappa \in (0, 1)$. The full discrete scheme as for (1.1) is: Find $z_N^m \in Y_N, m = 1, 2, \dots, K$, that satisfy the following equation:

$$\begin{aligned} & (\bar{A}_m z_N^0, v_N) + (\bar{B}_m z_N^1, v_N) + (\bar{C}_m z_N^2, v_N) + \left(\sum_{l=1}^{m-1} (A_l z_N^{m-l-1} + B_l z_N^{m-l} + C_l z_N^{m-l+1}), v_N \right) \\ & + \kappa_0 (\Delta z_N^m, \Delta v_N) = \kappa_0 (f^m, v_N), m \geq 1, \end{aligned} \quad (2.4)$$

for $\forall v_N \in Y_N$, where we assume that $\left(\sum_{l=1}^{m-1} (A_l z_N^{m-l-1} + B_l z_N^{m-l} + C_l z_N^{m-l+1}), v_N \right) = 0$ for $m = 1, 2$.

Similar to [28], in order to further study the stability and the convergence of scheme (2.4), for $m \geq 3$, we rewrite scheme (2.4) as follows: $z_N^m \in Y_N, m = 1, 2, \dots, K$, and $\forall v_N \in Y_N$ such that

$$\begin{cases} (\bar{A}_m z_N^0, v_N) + (\bar{B}_m z_N^1, v_N) + (\bar{C}_m z_N^2, v_N) + \kappa_0 (\Delta z_N^m, \Delta v_N) = \kappa_0 (f^m, v_N), m = 1, 2, \\ (z_N^m, v_N) + \kappa_0 \beta_0^{-1} (\Delta z_N^m, \Delta v_N) = \left(\sum_{i=1}^m D_{m-i}^m z_N^{m-i}, v_N \right) + \kappa_0 \beta_0^{-1} (f^m, v_N), m \geq 3, \end{cases} \quad (2.5)$$

where $C_1 = \frac{2-\kappa}{2} + 1 = \frac{4-\kappa}{2}$ according to the coefficient expression of (2.1), so $\beta_0 = C_1$. For $m = 3$,

$$D_0^3 = -\beta_0^{-1} (\bar{A}_3 + A_2), D_1^3 = -\beta_0^{-1} (\bar{B}_3 + A_1 + B_2), D_2^3 = -\beta_0^{-1} (\bar{C}_3 + B_1 + C_2),$$

and for $m \geq 4$,

$$\begin{aligned} D_{m-1}^m &= -\beta_0^{-1} (B_1 + C_2), D_{m-2}^m = -\beta_0^{-1} (A_1 + B_2 + C_3), \\ D_{m-i}^m &= -\beta_0^{-1} (A_{i-1} + B_i + C_{i+1}), i = 3, 4, \dots, m-3, \\ D_2^m &= -\beta_0^{-1} (\bar{C}_m + A_{m-3} + B_{m-2} + C_{m-1}), D_1^m = -\beta_0^{-1} (\bar{B}_m + A_{m-2} + B_{m-1}), \\ D_0^m &= -\beta_0^{-1} (\bar{A}_m + A_{m-1}). \end{aligned}$$

3. Stability analysis and error estimation

In this section, we will strictly establish the stability and error estimation of scheme (2.5). First, the properties of the coefficients D_{m-i}^m are provided in the following Lemma 3.1.

Lemma 3.1. [28] For given $0 < \kappa < 1, m \geq 4$, the coefficients of scheme (2.5) satisfy the following conditions:

$$(1) \beta_0 = C_1 = \frac{4-\kappa}{2} \in \left(\frac{3}{2}, 2 \right);$$

$$(2) \sum_{i=1}^m D_{m-i}^m \equiv 1;$$

$$(3) D_{m-i}^m > 0, i = 3, \dots, m;$$

(4) $0 < D_{m-1}^m < \frac{4}{3}$;
 (5) $\exists \kappa_0 \in (0, 1)$, such that $D_{m-2}^m > 0$ if $\kappa \in (0, \kappa_0)$ and $D_{m-2}^m < 0$ if $\kappa \in (\kappa_0, 1)$;
 (6) $D_{m-2}^m + \frac{1}{4} (D_{m-1}^m)^2 > 0$.

Lemma 3.1 implies that the symbol of the coefficient D_{m-2}^m remains uncertain $\forall \kappa \in (0, 1)$. Therefore, it would be very difficult to analyze the stability of our proposed numerical scheme (2.4) by applying the classical method. Therefore, we want to use a technique to construct a new method such that all the coefficients of our scheme are positive. An unconditional stable numerical scheme is derived $\forall \kappa \in (0, 1)$. Consequently, based on the properties of the coefficients of (2.5) in Lemma 3.1, we denote

$$\rho = \frac{1}{2} D_{m-1}^m, m \geq 4.$$

By using the definition of ρ , rewrite the last row of (2.5) as follows:

$$\begin{aligned} & (z_N^m - \rho z_N^{m-1}, v_N) + \kappa_0 \beta_0^{-1} (\Delta z_N^m, \Delta v_N) \\ &= \rho (z_N^{m-1} - \rho z_N^{m-2}, v_N) + (\rho^2 + D_{m-2}^m) (z_N^{m-2} - \rho z_N^{m-3}, v_N) \\ & \quad + (\rho^3 + \rho D_{m-2}^m + D_{m-3}^m) (z_N^{m-3} - \rho z_N^{m-4}, v_N) + D_{m-4}^m (z_N^{m-4}, v_N) \\ & \quad + \cdots + D_0^m (z_N^0, v_N) + \kappa_0 \beta_0^{-1} (f^m, v_N) \\ &= \rho (z_N^{m-1} - \rho z_N^{m-2}, v_N) + (\rho^2 + D_{m-2}^m) (z_N^{m-2} - \rho z_N^{m-3}, v_N) \\ & \quad + (\rho^3 + \rho D_{m-2}^m + D_{m-3}^m) (z_N^{m-3} - \rho z_N^{m-4}, v_N) \\ & \quad + \cdots + (\rho^{m-2} + \rho^{m-3} D_{m-2}^m + \cdots + \rho D_3^m + D_2^m) (z_N^2 - \rho z_N^1, v_N) \\ & \quad + (\rho^{m-1} + \rho^{m-2} D_{m-2}^m + \cdots + \rho D_2^m + D_1^m) (z_N^1 - \rho z_N^0, v_N) \\ & \quad + (\rho^m + \rho^{m-1} D_{m-2}^m + \cdots + \rho D_1^m + D_0^m) (z_N^0, v_N) + \kappa_0 \beta_0^{-1} (f^m, v_N). \end{aligned}$$

Second, we denote

$$\begin{aligned} \bar{D}_{m-i}^m &= \rho^i + \sum_{j=2}^i \rho^{i-j} D_{m-j}^m, \quad i = 2, 3, 4, \dots, m, \\ \bar{z}_N^i &= z_N^i - \rho z_N^{i-1}, \quad i = 1, 2, \dots, m. \end{aligned} \tag{3.1}$$

As $m = 3$, we get

$$(\bar{z}_N^3, v_N) + \kappa_0 \beta_0^{-1} (\Delta z_N^3, \Delta v_N) = \bar{D}_2^3 (\bar{z}_N^2, v_N) + \bar{D}_1^3 (\bar{z}_N^1, v_N) + \bar{D}_0^3 (z_N^0, v_N) + \kappa_0 \beta_0^{-1} (f^3, v_N),$$

where

$$\bar{D}_2^3 = D_2^3 - \rho, \bar{D}_1^3 = \bar{D}_2^3 \rho + D_1^3, \bar{D}_0^3 = \bar{D}_1^3 \rho + D_0^3.$$

Therefore, (2.5) can be written in an equivalent form as follows: $z_N^m \in Y_N$, $m = 1, 2, \dots, K$, and $\forall v_N \in Y_N$, we have

$$\begin{cases} (\bar{A}_m z_N^0, v_N) + (\bar{B}_m z_N^1, v_N) + (\bar{C}_m z_N^2, v_N) + \kappa_0 (\Delta z_N^m, \Delta v_N) = \kappa_0 (f^m, v_N), m = 1, 2, \\ (\bar{z}_N^3, v_N) + \kappa_0 \beta_0^{-1} (\Delta z_N^3, \Delta v_N) = \left(\sum_{i=1}^3 \bar{D}_{3-i}^3 \bar{z}_N^{3-i}, v_N \right) + \kappa_0 \beta_0^{-1} (f^3, v_N), m = 3, \\ (\bar{z}_N^m, v_N) + \kappa_0 \beta_0^{-1} (\Delta z_N^m, \Delta v_N) = \left(\rho \bar{z}_N^{m-1} + \sum_{i=2}^{m-1} \bar{D}_{m-i}^m \bar{z}_N^{m-i} + \bar{D}_0^m z_N^0, v_N \right) + \kappa_0 \beta_0^{-1} (f^m, v_N), m \geq 4. \end{cases} \tag{3.2}$$

Before analyzing scheme (3.2)'s stability, we will give the good properties of the coefficients, as detailed in the following Lemma 3.2.

Lemma 3.2. [28] For given $0 < \kappa < 1$, the coefficients in the 2nd–3rd rows of (3.2) satisfy the following conditions:

- (1) $0 < \rho < \frac{2}{3}$; (2) $\bar{D}_{m-i}^m > 0, 2 \leq i \leq m$;
- (3) $\rho + \sum_{i=2}^{m-1} \bar{D}_{m-i}^m + \bar{D}_0^m \leq 1$;
- (4) $\frac{1}{\bar{D}_0^m} < \frac{1}{D_0^m} < \frac{m^\kappa}{(1-\kappa)(2-\kappa)}$;
- (5) $\bar{D}_{3-i}^3 > 0, i = 1, 2, 3$;
- (6) $\bar{D}_2^3 + \bar{D}_1^3 + \bar{D}_0^3 \leq 1$;
- (7) $\bar{D}_2^3 - \rho \leq 0$.

Third, we analyze the stability of the Legendre-Galerkin spectral scheme (2.4).

Theorem 3.1. Suppose $\{z_N^m\}_{m=1}^K$ is the numerical solution of (2.4), and this numerical solution satisfies

$$\|z_N^m\|_0 + \sqrt{\kappa_0 \beta_0^{-1}} \|\Delta z_N^m\|_0 \leq 4 \left(H_1 \|z_N^0\|_0^2 + H_2 C_f [\Gamma(1-\kappa)]^2 T^{2\kappa} \max_{1 \leq i \leq K} \|f^i\|_0^2 \right)^{\frac{1}{2}}, \quad 1 \leq m \leq K, \quad (3.3)$$

where $C_f > 0$ is a constant independent of N and τ , and

$$H_1 = \max \{2(M_1 + \rho^2), 2(M_3 + \rho^2 M_1)\}, \quad H_2 = \max \{2M_2, 2(M_4 + \rho^2 M_2)\}. \quad (3.4)$$

The expressions of $M_i (i = 1, 2, 3, 4)$ are as follows:

$$\begin{aligned} M_1 &= \frac{(15\kappa - 18)(\kappa - 2)}{8(1-\kappa)^2(\kappa+2)}, \quad M_2 = (2-\kappa)^2 \left[\frac{1}{2} + \frac{4^\kappa(1-\kappa)}{8(\kappa+2)} \right], \\ M_3 &= \frac{2(15\kappa - 18)(\kappa - 2)}{(1-\kappa)(\kappa+2)^2}, \quad M_4 = (1-\kappa)(2-\kappa)^2 \left[\frac{2 \cdot 4^\kappa(1-\kappa)}{(\kappa+2)^2} + \frac{8}{(\kappa+2)} \right]. \end{aligned} \quad (3.5)$$

Proof. Let $v_N = -\bar{B}_2 z_N^1$ in (3.2) for $m = 1$ and $v_N = \bar{C}_1 z_N^2$ in (3.2) for $m = 2$. Adding them, we have

$$\begin{aligned} &-\bar{B}_1 \bar{B}_2 \|z_N^1\|_0^2 + \bar{C}_1 \bar{C}_2 \|z_N^2\|_0^2 - \kappa_0 \bar{B}_2 \|\Delta z_N^1\|_0^2 + \kappa_0 \bar{C}_1 \|\Delta z_N^2\|_0^2 \\ &= -\kappa_0 \bar{B}_2 (f^1, z_N^1) + \kappa_0 \bar{C}_1 (f^2, z_N^2) + \bar{A}_1 \bar{B}_2 (z_N^0, z_N^1) - \bar{C}_1 \bar{A}_2 (z_N^0, z_N^2). \end{aligned}$$

By Young's inequality, we obtain

$$\begin{aligned} &-\bar{B}_1 \bar{B}_2 \|z_N^1\|_0^2 + \bar{C}_1 \bar{C}_2 \|z_N^2\|_0^2 - \kappa_0 \bar{B}_2 \|\Delta z_N^1\|_0^2 + \kappa_0 \bar{C}_1 \|\Delta z_N^2\|_0^2 \\ &\leq \frac{1}{2} \frac{(-\kappa_0 \bar{B}_2)^2}{\varepsilon_1} \|f^1\|_0^2 + \frac{\varepsilon_1}{2} \|z_N^1\|_0^2 + \frac{1}{2} \frac{(\kappa_0 \bar{C}_1)^2}{\varepsilon_2} \|f^2\|_0^2 + \frac{\varepsilon_2}{2} \|z_N^2\|_0^2 \\ &\quad + \frac{1}{2} \frac{(\bar{A}_1 \bar{B}_2)^2}{\varepsilon_1} \|z_N^0\|_0^2 + \frac{\varepsilon_1}{2} \|z_N^1\|_0^2 + \frac{1}{2} \frac{(-\bar{C}_1 \bar{A}_2)^2}{\varepsilon_2} \|z_N^0\|_0^2 + \frac{\varepsilon_2}{2} \|z_N^2\|_0^2. \end{aligned}$$

Let us denote $\varepsilon_1 = -\frac{\bar{B}_1\bar{B}_2}{2}$, $\varepsilon_2 = \frac{\bar{C}_1\bar{C}_2}{2}$ and substitute them into the above inequality:

$$\begin{aligned} & -\frac{1}{2}\bar{B}_1\bar{B}_2\|z_N^1\|_0^2 + \frac{1}{2}\bar{C}_1\bar{C}_2\|z_N^2\|_0^2 - \kappa_0\bar{B}_2\|\Delta z_N^1\|_0^2 + \kappa_0\bar{C}_1\|\Delta z_N^2\|_0^2 \\ & \leq -\frac{(-\kappa_0\bar{B}_2)^2}{\bar{B}_1\bar{B}_2}\|f^1\|_0^2 + \frac{(\kappa_0\bar{C}_1)^2}{\bar{C}_1\bar{C}_2}\|f^2\|_0^2 - \frac{(\bar{A}_1\bar{B}_2)^2}{\bar{B}_1\bar{B}_2}\|z_N^0\|_0^2 + \frac{(-\bar{A}_2\bar{C}_1)^2}{\bar{C}_1\bar{C}_2}\|z_N^0\|_0^2. \end{aligned} \quad (3.6)$$

Simplifying the above inequality (3.6), we have

$$\begin{aligned} & -\bar{B}_1\bar{B}_2\|z_N^1\|_0^2 + \bar{C}_1\bar{C}_2\|z_N^2\|_0^2 - 2\kappa_0\bar{B}_2\|\Delta z_N^1\|_0^2 + 2\kappa_0\bar{C}_1\|\Delta z_N^2\|_0^2 \\ & \leq \frac{2(-\kappa_0\bar{B}_2)^2}{-\bar{B}_1\bar{B}_2}\|f^1\|_0^2 + \frac{2(\kappa_0\bar{C}_1)^2}{\bar{C}_1\bar{C}_2}\|f^2\|_0^2 + 2\left[\frac{(\bar{A}_1\bar{B}_2)^2}{-\bar{B}_1\bar{B}_2} + \frac{(-\bar{A}_2\bar{C}_1)^2}{\bar{C}_1\bar{C}_2}\right]\|z_N^0\|_0^2. \end{aligned} \quad (3.7)$$

Arranging the inequality (3.7), we can get

$$\begin{aligned} & -\bar{B}_1\bar{B}_2\|z_N^1\|_0^2 - 2\kappa_0\bar{B}_2\|\Delta z_N^1\|_0^2 \\ & \leq 2\left(\frac{\bar{A}_2^2\bar{C}_1\bar{B}_1 - \bar{A}_1^2\bar{B}_2\bar{C}_2}{\bar{B}_1\bar{C}_2}\right)\|z_N^0\|_0^2 + \frac{2(-\kappa_0\bar{B}_2)^2}{-\bar{B}_1\bar{B}_2}\|f^1\|_0^2 + \frac{2(\kappa_0\bar{C}_1)^2}{\bar{C}_1\bar{C}_2}\|f^2\|_0^2. \end{aligned}$$

Both sides of the inequality on the previous line are divided by $-\bar{B}_1\bar{B}_2$, and we obtain

$$\begin{aligned} & \|z_N^1\|_0^2 + \frac{2\kappa_0}{\bar{B}_1}\|\Delta z_N^1\|_0^2 \\ & \leq \left[\frac{2(\bar{A}_2^2\bar{C}_1\bar{B}_1 - \bar{A}_1^2\bar{B}_2\bar{C}_2)}{\bar{B}_1\bar{C}_2}\|z_N^0\|_0^2 + \frac{2(-\kappa_0\bar{B}_2)^2}{-\bar{B}_1\bar{B}_2}\|f^1\|_0^2 + \frac{2(\kappa_0\bar{C}_1)^2}{\bar{C}_1\bar{C}_2}\|f^2\|_0^2\right]/(-\bar{B}_1\bar{B}_2). \end{aligned}$$

From the characteristics of \bar{B}_1 and β_0 , we have $\bar{B}_1 < 2\beta_0$. From the previous inequality, we obtain

$$\begin{aligned} & \|z_N^1\|_0^2 + \kappa_0\beta_0^{-1}\|\Delta z_N^1\|_0^2 < \|z_N^1\|_0^2 + \frac{2\kappa_0}{\bar{B}_1}\|\Delta z_N^1\|_0^2 \\ & \leq \frac{2(\bar{A}_1^2\bar{B}_2\bar{C}_2 - \bar{A}_2^2\bar{C}_1\bar{B}_1)}{\bar{B}_1^2\bar{C}_2\bar{B}_2}\|z_N^0\|_0^2 + \left[\frac{2(-\kappa_0\bar{B}_2)^2}{-\bar{B}_1\bar{B}_2} + \frac{2(\kappa_0\bar{C}_1)^2}{\bar{C}_1\bar{C}_2}\right]/(-\bar{B}_1\bar{B}_2)\max_{i=1,2}\|f^i\|_0^2 \\ & = M_1\|z_N^0\|_0^2 + M_2[\Gamma(1-\kappa)]^2T^{2\kappa}\max_{i=1,2}\|f^i\|_0^2, \end{aligned}$$

where M_1, M_2 are defined in (3.5).

Therefore, $\bar{z}_N^1 = z_N^1 - \rho z_N^0$ and $0 < \rho < \frac{2}{3}$, when $m = 1$, and we obtain

$$\begin{aligned} & \|\bar{z}_N^1\|_0^2 + \kappa_0\beta_0^{-1}\|\Delta z_N^1\|_0^2 = \|z_N^1 - \rho z_N^0\|_0^2 + \kappa_0\beta_0^{-1}\|\Delta z_N^1\|_0^2 \\ & = (z_N^1, z_N^1) - \rho(z_N^1, z_N^0) - \rho(z_N^0, z_N^1) + \rho^2(z_N^0, z_N^0) + \kappa_0\beta_0^{-1}\|\Delta z_N^1\|_0^2 \\ & \leq \|z_N^1\|_0^2 + 2\rho\|z_N^1\|_0\|z_N^0\|_0 + \rho^2\|z_N^0\|_0^2 + \kappa_0\beta_0^{-1}\|\Delta z_N^1\|_0^2 \\ & \leq 2(\|z_N^1\|_0^2 + \kappa_0\beta_0^{-1}\|\Delta z_N^1\|_0^2) + 2\rho^2\|z_N^0\|_0^2 \\ & \leq 2(M_1\|z_N^0\|_0^2 + M_2[\Gamma(1-\kappa)]^2T^{2\kappa}\max_{i=1,2}\|f^i\|_0^2) + 2\rho^2\|z_N^0\|_0^2 \end{aligned}$$

$$= 2(M_1 + \rho^2) \|z_N^0\|_0^2 + 2M_2[\Gamma(1 - \kappa)]^2 T^{2\kappa} \max_{i=1,2} \|f^i\|_0^2. \quad (3.8)$$

Similarly, it can be seen from (3.7) that

$$\begin{aligned} \|z_N^2\|_0^2 + \kappa_0 \beta_0^{-1} \|\Delta z_N^2\|_0^2 &\leq \|z_N^2\|_0^2 + \frac{2\kappa_0}{\bar{C}_2} \|\Delta z_N^2\|_0^2 \\ &\leq \frac{2(\bar{A}_2^2 \bar{B}_1 \bar{C}_1 - \bar{A}_1^2 \bar{B}_2 \bar{C}_2)}{\bar{B}_1 \bar{C}_2^2 \bar{C}_1} \|z_N^0\|_0^2 + \left[\frac{2(-\kappa_0 \bar{B}_2)^2}{-\bar{B}_1 \bar{B}_2} + \frac{2(\kappa_0 \bar{C}_1)^2}{\bar{C}_1 \bar{C}_2} \right] / (\bar{C}_1 \bar{C}_2) \max_{i=1,2} \|f^i\|_0^2 \\ &= M_3 \|z_N^0\|_0^2 + M_4 [\Gamma(1 - \kappa)]^2 T^{2\kappa} \max_{i=1,2} \|f^i\|_0^2, \end{aligned}$$

where M_3, M_4 are defined in (3.5).

Then $m = 2$, $\bar{z}_N^2 = z_N^2 - \rho z_N^1$, and

$$\begin{aligned} \|\bar{z}_N^2\|_0^2 + \kappa_0 \beta_0^{-1} \|\Delta z_N^2\|_0^2 &= \|z_N^2 - \rho z_N^1\|_0^2 + \kappa_0 \beta_0^{-1} \|\Delta z_N^2\|_0^2 \\ &= (z_N^2, z_N^2) - \rho(z_N^2, z_N^1) - \rho(z_N^1, z_N^2) + \rho^2(z_N^1, z_N^1) + \kappa_0 \beta_0^{-1} \|\Delta z_N^2\|_0^2 \\ &\leq \|z_N^2\|_0^2 + 2\rho \|z_N^2\|_0 \|z_N^1\|_0^2 + \rho^2 \|z_N^1\|_0^2 + \kappa_0 \beta_0^{-1} \|\Delta z_N^2\|_0^2 \\ &\leq 2(\|z_N^2\|_0^2 + \kappa_0 \beta_0^{-1} \|\Delta z_N^2\|_0^2) + 2\rho^2(\|z_N^1\|_0^2 + \kappa_0 \beta_0^{-1} \|\Delta z_N^1\|_0^2) \\ &\leq 2(M_3 \|z_N^0\|_0^2 + M_4 [\Gamma(1 - \kappa)]^2 T^{2\kappa} \max_{i=1,2} \|f^i\|_0^2) \\ &\quad + 2\rho^2(M_1 \|z_N^0\|_0^2 + M_2 [\Gamma(1 - \kappa)]^2 T^{2\kappa} \max_{i=1,2} \|f^i\|_0^2) \\ &= 2(M_3 + \rho^2 M_1) \|z_N^0\|_0^2 + 2(M_4 + \rho^2 M_2) [\Gamma(1 - \kappa)]^2 T^{2\kappa} \max_{i=1,2} \|f^i\|_0^2. \quad (3.9) \end{aligned}$$

For (3.8) and (3.9), we have

$$\|\bar{z}_N^1\|_0^2 + \kappa_0 \beta_0^{-1} \|\Delta z_N^1\|_0^2 \leq H_1 \|z_N^0\|_0^2 + H_2 [\Gamma(1 - \kappa)]^2 T^{2\kappa} \max_{i=1,2} \|f^i\|_0^2, \quad (3.10)$$

$$\|\bar{z}_N^2\|_0^2 + \kappa_0 \beta_0^{-1} \|\Delta z_N^2\|_0^2 \leq H_1 \|z_N^0\|_0^2 + H_2 [\Gamma(1 - \kappa)]^2 T^{2\kappa} \max_{i=1,2} \|f^i\|_0^2, \quad (3.11)$$

where H_1, H_2 are defined in (3.4).

When $m \geq 3$, letting $v_N = 2\bar{z}_N^m$ in (3.2), we get

$$\begin{aligned} 2 \|\bar{z}_N^m\|_0^2 + 2\kappa_0 \beta_0^{-1} (\Delta z_N^m, \Delta \bar{z}_N^m) \\ = 2\rho(\bar{z}_N^{m-1}, \bar{z}_N^m) + 2 \sum_{i=2}^{m-1} \bar{D}_{m-i}^m(\bar{z}_N^{m-i}, \bar{z}_N^m) + 2\bar{D}_0^m(z_N^0, \bar{z}_N^m) + 2\kappa_0 \beta_0^{-1} (f^m, \bar{z}_N^m). \end{aligned}$$

Using $2(\Delta z_N^m, \Delta \bar{z}_N^m) = \|\Delta z_N^m\|_0^2 + \|\Delta \bar{z}_N^m\|_0^2 - \rho^2 \|\Delta z_N^{m-1}\|_0^2$ and integration by parts, we have

$$\begin{aligned} 2 \|\bar{z}_N^m\|_0^2 + \kappa_0 \beta_0^{-1} \|\Delta z_N^m\|_0^2 + \kappa_0 \beta_0^{-1} \|\Delta \bar{z}_N^m\|_0^2 - \kappa_0 \beta_0^{-1} \rho^2 \|\Delta z_N^{m-1}\|_0^2 \\ = 2\rho(\bar{z}_N^{m-1}, \bar{z}_N^m) + 2 \sum_{i=2}^{m-1} \bar{D}_{m-i}^m(\bar{z}_N^{m-i}, \bar{z}_N^m) + 2\bar{D}_0^m(z_N^0, \bar{z}_N^m) + 2\kappa_0 \beta_0^{-1} (f^m, \bar{z}_N^m) \end{aligned}$$

$$= 2\rho(\bar{z}_N^{m-1}, \bar{z}_N^m) + 2 \sum_{i=2}^{m-1} \bar{D}_{m-i}^m(\bar{z}_N^{m-i}, \bar{z}_N^m) + 2\bar{D}_0^m(z_N^0, \bar{z}_N^m) + 2\kappa_0\beta_0^{-1}((\Delta)^{-1}f^m, \Delta\bar{z}_N^m),$$

where $(\Delta)^{-1}$ is the inverse operator of Δ .

By using the basic inequality, we obtain

$$\begin{aligned} & 2\|\bar{z}_N^m\|_0^2 + \kappa_0\beta_0^{-1}\|\Delta z_N^m\|_0^2 + \kappa_0\beta_0^{-1}\|\Delta\bar{z}_N^m\|_0^2 - \kappa_0\beta_0^{-1}\rho^2\|\Delta z_N^{m-1}\|_0^2 \\ & \leq \rho\left(\|\bar{z}_N^{m-1}\|_0^2 + \|\bar{z}_N^m\|_0^2\right) + \sum_{i=2}^{m-1} \bar{D}_{m-i}^m\left(\|\bar{z}_N^{m-i}\|_0^2 + \|\bar{z}_N^m\|_0^2\right) + \bar{D}_0^m\left(\|z_N^0\|_0^2 + \|\bar{z}_N^m\|_0^2\right) \\ & \quad + \kappa_0\beta_0^{-1}\|(\Delta)^{-1}f^m\|_0^2 + \kappa_0\beta_0^{-1}\|\Delta\bar{z}_N^m\|_0^2. \end{aligned} \quad (3.12)$$

By rearranging (3.12), we immediately obtain

$$\begin{aligned} & 2\|\bar{z}_N^m\|_0^2 + \kappa_0\beta_0^{-1}\|\Delta z_N^m\|_0^2 - \kappa_0\beta_0^{-1}\rho^2\|\Delta z_N^{m-1}\|_0^2 \\ & \leq \rho\|\bar{z}_N^{m-1}\|_0^2 + \left(\rho + \bar{D}_0^m + \sum_{i=2}^{m-1} \bar{D}_{m-i}^m\right)\|\bar{z}_N^m\|_0^2 \\ & \quad + \sum_{i=2}^{m-1} \bar{D}_{m-i}^m\|\bar{z}_N^{m-i}\|_0^2 + \bar{D}_0^m\|z_N^0\|_0^2 + \kappa_0\beta_0^{-1}\|(\Delta)^{-1}f^m\|_0^2. \end{aligned}$$

From (5)–(7) in Lemma 3.2, we can observe that the above inequality satisfies for $m = 3$. Through detailed calculation, it can be inferred that $\rho + \bar{D}_1^3 + \bar{D}_2^3 \leq 1$. From (3) in Lemma 3.2, we have $\rho + \sum_{i=2}^{m-1} \bar{D}_{m-i}^m + \bar{D}_0^m \leq 1$, and then

$$\begin{aligned} & \|\bar{z}_N^m\|_0^2 + \kappa_0\beta_0^{-1}\|\Delta z_N^m\|_0^2 - \kappa_0\beta_0^{-1}\rho^2\|\Delta z_N^{m-1}\|_0^2 \\ & \leq \rho\|\bar{z}_N^{m-1}\|_0^2 + \sum_{i=2}^{m-1} \bar{D}_{m-i}^m\|\bar{z}_N^{m-i}\|_0^2 + \bar{D}_0^m\|z_N^0\|_0^2 + \kappa_0\beta_0^{-1}\|(\Delta)^{-1}f^m\|_0^2. \end{aligned}$$

According to (1) and (4) in Lemma 3.2 and $\frac{3}{2} < \beta_0 < 2$ in Lemma 3.1, we get

$$\begin{aligned} & \|\bar{z}_N^m\|_0^2 + \kappa_0\beta_0^{-1}\|\Delta z_N^m\|_0^2 \\ & \leq \rho\left(\|\bar{z}_N^{m-1}\|_0^2 + \kappa_0\beta_0^{-1}\rho\|\Delta z_N^{m-1}\|_0^2\right) + \sum_{i=2}^{m-1} \bar{D}_{m-i}^m\|\bar{z}_N^{m-i}\|_0^2 + \bar{D}_0^m\|z_N^0\|_0^2 + \kappa_0\beta_0^{-1}\|(\Delta)^{-1}f^m\|_0^2 \\ & \leq \rho\left(\|\bar{z}_N^{m-1}\|_0^2 + \kappa_0\beta_0^{-1}\rho\|\Delta z_N^{m-1}\|_0^2\right) + \sum_{i=2}^{m-1} \bar{D}_{m-i}^m\left(\|\bar{z}_N^{m-i}\|_0^2 + \kappa_0\beta_0^{-1}\|\Delta z_N^{m-i}\|_0^2\right) \\ & \quad + \bar{D}_0^m\left(\|z_N^0\|_0^2 + \frac{\kappa_0}{\bar{D}_0^m\beta_0}\|(\Delta)^{-1}f^m\|_0^2\right) \\ & \leq \rho\left(\|\bar{z}_N^{m-1}\|_0^2 + \kappa_0\beta_0^{-1}\rho\|\Delta z_N^{m-1}\|_0^2\right) + \sum_{i=2}^{m-1} \bar{D}_{m-i}^m\left(\|\bar{z}_N^{m-i}\|_0^2 + \kappa_0\beta_0^{-1}\|\Delta z_N^{m-i}\|_0^2\right) \end{aligned}$$

$$\begin{aligned}
& + \bar{D}_0^m \left(\|z_N^0\|_0^2 + \frac{\kappa_0 \cdot m^\kappa}{(1-\kappa)(2-\kappa)\beta_0} \|(\Delta)^{-1} f^m\|_0^2 \right) \\
& \leq \rho \left(\|\bar{z}_N^{m-1}\|_0^2 + \kappa_0 \beta_0^{-1} \rho \|\Delta z_N^{m-1}\|_0^2 \right) + \sum_{i=2}^{m-1} \bar{D}_{m-i}^m \left(\|\bar{z}_N^{m-i}\|_0^2 + \kappa_0 \beta_0^{-1} \|\Delta z_N^{m-i}\|_0^2 \right) \\
& \quad + \bar{D}_0^m \left(\|z_N^0\|_0^2 + \frac{\Gamma(1-\kappa)T^\kappa}{\beta_0} \|(\Delta)^{-1} f^m\|_0^2 \right) \\
& \leq \rho \left(\|\bar{z}_N^{m-1}\|_0^2 + \kappa_0 \beta_0^{-1} \rho \|\Delta z_N^{m-1}\|_0^2 \right) + \sum_{i=2}^{m-1} \bar{D}_{m-i}^m \left(\|\bar{z}_N^{m-i}\|_0^2 + \kappa_0 \beta_0^{-1} \|\Delta z_N^{m-i}\|_0^2 \right) \\
& \quad + \bar{D}_0^m \left(\|z_N^0\|_0^2 + \frac{\Gamma(1-\kappa)T^\kappa C_f}{\beta_0} \|f^m\|_0^2 \right) \\
& \leq \rho \left(\|\bar{z}_N^{m-1}\|_0^2 + \kappa_0 \beta_0^{-1} \|\Delta z_N^{m-1}\|_0^2 \right) + \sum_{i=2}^{m-1} \bar{D}_{m-i}^m \left(\|\bar{z}_N^{m-i}\|_0^2 + \kappa_0 \beta_0^{-1} \|\Delta z_N^{m-i}\|_0^2 \right) \\
& \quad + \bar{D}_0^m \left(\|z_N^0\|_0^2 + C_f \Gamma(1-\kappa) T^\kappa \|f^m\|_0^2 \right), \tag{3.13}
\end{aligned}$$

where $C_f > 0$ and depends on the function f .

To prove the following estimate, we will adopt mathematical induction:

$$\|\bar{z}_N^m\|_0^2 + \kappa_0 \beta_0^{-1} \|\Delta z_N^m\|_0^2 \leq H_1 \|z_N^0\|_0^2 + H_2 C_f [\Gamma(1-\kappa)]^2 T^{2\kappa} \max_{1 \leq i \leq K} \|f^i\|_0^2, \quad m \geq 3. \tag{3.14}$$

According to (3.10) and (3.11), (3.14) is obviously valid for $m = 1, 2$. It can be easily proved that (3.14) holds when $m = 3$. We assume that (3.14) also hold for $j = 3, 4, \dots, m-1$,

$$\|\bar{z}_N^j\|_0^2 + \kappa_0 \beta_0^{-1} \|\Delta z_N^j\|_0^2 \leq H_1 \|z_N^0\|_0^2 + H_2 C_f [\Gamma(1-\kappa)]^2 T^{2\kappa} \max_{1 \leq i \leq K} \|f^i\|_0^2, \quad 1 \leq j \leq m-1.$$

We deduce from (3.13) that

$$\|\bar{z}_N^m\|_0^2 + \kappa_0 \beta_0^{-1} \|\Delta z_N^m\|_0^2 \leq \left(\rho + \sum_{i=2}^{m-1} \bar{D}_{m-i}^m + \bar{D}_0^m \right) \left(H_1 \|z_N^0\|_0^2 + H_2 C_f [\Gamma(1-\kappa)]^2 T^{2\kappa} \max_{1 \leq i \leq K} \|f^i\|_0^2 \right).$$

According to (3.14), we can obtain

$$\sqrt{\kappa_0 \beta_0^{-1}} \|\Delta z_N^m\|_0 \leq \left(H_1 \|z_N^0\|_0^2 + H_2 C_f [\Gamma(1-\kappa)]^2 T^{2\kappa} \max_{1 \leq i \leq K} \|f^i\|_0^2 \right)^{\frac{1}{2}}, \tag{3.15}$$

$$\|\bar{z}_N^m\|_0 \leq \left(H_1 \|z_N^0\|_0^2 + H_2 C_f [\Gamma(1-\kappa)]^2 T^{2\kappa} \max_{1 \leq i \leq K} \|f^i\|_0^2 \right)^{\frac{1}{2}}. \tag{3.16}$$

Finally, by (3.16) and the triangle inequality to estimate $\|z_N^m\|_0$, we obtain

$$\begin{aligned}
\|z_N^m\|_0 &= \|\bar{z}_N^m + \rho z_N^{m-1}\|_0 \\
&\leq \rho \|z_N^{m-1}\|_0 + \left(H_1 \|z_N^0\|_0^2 + H_2 C_f [\Gamma(1-\kappa)]^2 T^{2\kappa} \max_{1 \leq i \leq K} \|f^i\|_0^2 \right)^{\frac{1}{2}} \\
&\leq \rho \left[\rho \|z_N^{m-2}\|_0 + (H_1 \|z_N^0\|_0^2 + H_2 C_f [\Gamma(1-\kappa)]^2 T^{2\kappa} \max_{1 \leq i \leq K} \|f^i\|_0^2)^{\frac{1}{2}} \right]
\end{aligned}$$

$$\begin{aligned}
& + \left(H_1 \|z_N^0\|_0^2 + H_2 C_f [\Gamma(1-\kappa)]^2 T^{2\kappa} \max_{1 \leq i \leq K} \|f^i\|_0^2 \right)^{\frac{1}{2}} \\
& \leq \dots \leq (1 + \rho + \dots + \rho^{m-2} + \rho^{m-1}) \left(H_1 \|z_N^0\|_0^2 + H_2 C_f [\Gamma(1-\kappa)]^2 T^{2\kappa} \max_{1 \leq i \leq K} \|f^i\|_0^2 \right)^{\frac{1}{2}} \\
& \leq \frac{1 - \rho^m}{1 - \rho} \left(H_1 \|z_N^0\|_0^2 + H_2 C_f [\Gamma(1-\kappa)]^2 T^{2\kappa} \max_{1 \leq i \leq K} \|f^i\|_0^2 \right)^{\frac{1}{2}} \\
& \leq 3 \left(H_1 \|z_N^0\|_0^2 + H_2 C_f [\Gamma(1-\kappa)]^2 T^{2\kappa} \max_{1 \leq i \leq K} \|f^i\|_0^2 \right)^{\frac{1}{2}}.
\end{aligned}$$

Therefore we obtain

$$\|z_N^m\|_0 + \sqrt{\kappa_0 \beta_0^{-1}} \|\Delta z_N^m\|_0 \leq 4 \left(H_1 \|z_N^0\|_0^2 + H_2 C_f [\Gamma(1-\kappa)]^2 T^{2\kappa} \max_{1 \leq i \leq K} \|f^i\|_0^2 \right)^{\frac{1}{2}}, \quad (3.17)$$

for $m = 1, 2, \dots, K$.

The proof is complete. \square

Lemma 3.3. [4] Define the projection operator $\mathbb{K}_{2,N}^0 : Y \mapsto Y_N$ which satisfies for any $\mu \in Y$ that

$$(\Delta(\mu - \mathbb{K}_{2,N}^0 \mu), \Delta v_N) = 0, \quad \forall v_N \in Y_N.$$

Then for any $\mu \in H^q(\Omega) \cap Y$ and $q \geq 2$, we have

$$\|\mu - \mathbb{K}_{2,N}^0 \mu\|_k \leq C N^{k-q} \|\mu\|_q, \quad k = 0, 1, 2.$$

Theorem 3.2. Let $z(\mathbf{x}, t)$ and $z_N^m, m = 1, 2, \dots, K$, be the exact solution and the approximate solution of (1.2) and (2.5), respectively. Assume that $z(\cdot, t) \in C^4[0, T]$ and $z(\mathbf{x}, \cdot) \in H^q(\Omega) \cap Y, q \geq 2$. Then we can obtain the following error estimation:

$$\|z_N^m - z(\mathbf{x}, t_m)\|_2 \leq C(\tau^{3-\kappa} + N^{2-q}), \quad m = 1, 2, \dots, K,$$

where C is a positive constant independent of N and τ .

Proof. Denote

$$z_N^m - z(\mathbf{x}, t_m) = z_N^m - \mathbb{K}_{2,N}^0 z(\mathbf{x}, t_m) + \mathbb{K}_{2,N}^0 z(\mathbf{x}, t_m) - z(\mathbf{x}, t_m) = \theta^m + \eta^m, \quad (3.18)$$

where $\theta^m = z_N^m - \mathbb{K}_{2,N}^0 z(\mathbf{x}, t_m)$, $\eta^m = \mathbb{K}_{2,N}^0 z(\mathbf{x}, t_m) - z(\mathbf{x}, t_m)$, for $m = 1, 2, \dots, K$.

When $m = 1, 2$, from the definition of $\mathbb{K}_{2,N}^0$ and (2.2), $\forall v_N \in Y_N$, we have

$$\bar{A}_m(z(\mathbf{x}, t_0), v_N) + \bar{B}_m(z(\mathbf{x}, t_1), v_N) + \bar{C}_m(z(\mathbf{x}, t_2), v_N) + \kappa_0(\Delta \mathbb{K}_{2,N}^0 z(\mathbf{x}, t_m), \Delta v_N) = \kappa_0(f^m, v_N) - \kappa_0(R_\tau^m, v_N).$$

By subtracting the corresponding formula in (2.5) for $m = 1, 2$, we can obtain:

$$\bar{A}_m(\theta^0 + \eta^0, v_N) + \bar{B}_m(\theta^1 + \eta^1, v_N) + \bar{C}_m(\theta^2 + \eta^2, v_N) + \kappa_0(\Delta \theta^m, \Delta v_N) = \kappa_0(R_\tau^m, v_N). \quad (3.19)$$

Let $v_N = -\bar{B}_2 \theta^1$ in (3.19) for $m = 1$, $v_N = \bar{C}_1 \theta^2$ in (3.19) for $m = 2$, and add them. Then, using Young's inequality, we get

$$-\bar{B}_1 \bar{B}_2 \|\theta^1\|_0^2 + \bar{C}_1 \bar{C}_2 \|\theta^2\|_0^2 - \kappa_0 \bar{B}_2 \|\Delta \theta^1\|_0^2 + \kappa_0 \bar{C}_1 \|\Delta \theta^2\|_0^2$$

$$\begin{aligned}
&= -\kappa_0 \bar{B}_2(R_\tau^1, \theta^1) + \kappa_0 \bar{C}_1(R_\tau^2, \theta^2) + \bar{A}_1 \bar{B}_2(\eta^0, \theta^1) + \bar{B}_1 \bar{B}_2(\eta^1, \theta^1) + \bar{C}_1 \bar{B}_2(\eta^2, \theta^1) \\
&\quad - \bar{C}_1 \bar{A}_2(\eta^0, \theta^2) - \bar{C}_1 \bar{B}_2(\eta^1, \theta^2) - \bar{C}_1 \bar{C}_2(\eta^2, \theta^2) + \bar{A}_1 \bar{B}_2(\theta^0, \theta^1) - \bar{C}_1 \bar{A}_2(\theta^0, \theta^2) \\
&\leq \frac{(-\kappa_0 \bar{B}_2)^2}{2\varepsilon_1} \|R_\tau^1\|_0^2 + \frac{(\kappa_0 \bar{C}_1)^2}{2\varepsilon_2} \|R_\tau^2\|_0^2 + \left[\frac{(\bar{B}_2 \bar{A}_1)^2}{2\varepsilon_1} + \frac{(-\bar{A}_2 \bar{C}_1)^2}{2\varepsilon_2} \right] \|\theta^0\|_0^2 \\
&\quad + \frac{5\varepsilon_1}{2} \|\theta^1\|_0^2 + \frac{5\varepsilon_2}{2} \|\theta^2\|_0^2 + \left[\frac{(\bar{B}_2 \bar{A}_1)^2}{2\varepsilon_1} + \frac{(-\bar{A}_2 \bar{C}_1)^2}{2\varepsilon_2} \right] \|\eta^0\|_0^2 \\
&\quad + \left[\frac{(\bar{B}_1 \bar{B}_2)^2}{2\varepsilon_1} + \frac{(-\bar{B}_2 \bar{C}_1)^2}{2\varepsilon_2} \right] \|\eta^1\|_0^2 + \left[\frac{(\bar{B}_2 \bar{C}_1)^2}{2\varepsilon_1} + \frac{(-\bar{C}_2 \bar{C}_1)^2}{2\varepsilon_2} \right] \|\eta^2\|_0^2. \tag{3.20}
\end{aligned}$$

Let $\varepsilon_1 = -\frac{\bar{B}_1 \bar{B}_2}{5}$, $\varepsilon_2 = \frac{\bar{C}_1 \bar{C}_2}{5}$ in (3.20), and we get

$$\begin{aligned}
&-\bar{B}_1 \bar{B}_2 \|\theta^1\|_0^2 + \bar{C}_2 \bar{C}_1 \|\theta^2\|_0^2 - 2\kappa_0 \bar{B}_2 \|\Delta \theta^1\|_0^2 + 2\kappa_0 \bar{C}_1 \|\Delta \theta^2\|_0^2 \\
&\leq \frac{5(-\kappa_0 \bar{B}_2)^2}{-\bar{B}_2 \bar{B}_1} \|R_\tau^1\|_0^2 + \frac{5(\kappa_0 \bar{C}_1)^2}{\bar{C}_1 \bar{C}_2} \|R_\tau^2\|_0^2 + 5 \frac{\bar{A}_2^2 \bar{B}_1 \bar{C}_1 - \bar{A}_1^2 \bar{B}_2 \bar{C}_2}{\bar{B}_1 \bar{C}_2} \|\theta^0\|_0^2 \\
&\quad + 5 \frac{\bar{A}_2^2 \bar{B}_1 \bar{C}_1 - \bar{A}_1^2 \bar{B}_2 \bar{C}_2}{\bar{B}_1 \bar{C}_2} \|\eta^0\|_0^2 + 5 \frac{\bar{B}_2^2 \bar{C}_1 - \bar{B}_2 \bar{B}_1 \bar{C}_2}{\bar{C}_2} \|\eta^1\|_0^2 + 5 \frac{\bar{C}_2 \bar{C}_1 \bar{B}_1 - \bar{C}_1^2 \bar{B}_2}{\bar{B}_1} \|\eta^2\|_0^2. \tag{3.21}
\end{aligned}$$

According to (3.21), and Lemmas 2.1 and 3.3, inequality (3.21) becomes

$$\begin{aligned}
&\|\theta^1\|_0^2 + \kappa_0 \beta_0^{-1} \|\Delta \theta^1\|_0^2 < \|\theta^1\|_0^2 + \frac{2\kappa_0}{\bar{B}_1} \|\Delta \theta^1\|_0^2 \\
&\leq 5 \frac{\bar{A}_2^2 \bar{B}_1 \bar{C}_1 - \bar{A}_1^2 \bar{B}_2 \bar{C}_2}{\bar{B}_1 \bar{C}_2} \|\theta^0\|_0^2 + \left(\frac{5\kappa_0^2}{\bar{B}_1^2} - \frac{5\kappa_0^2 \bar{C}_1}{\bar{C}_2 \bar{B}_1 \bar{B}_2} \right) \max_{i=1,2} \|R_\tau^i\|_0^2 \\
&\quad + \left[5 \frac{\bar{A}_2^2 \bar{B}_1 \bar{C}_1 - \bar{A}_1^2 \bar{B}_2 \bar{C}_2}{\bar{B}_1 \bar{C}_2} \|\eta^0\|_0^2 + 5 \frac{\bar{B}_2^2 \bar{C}_1 - \bar{B}_2 \bar{B}_1 \bar{C}_2}{\bar{C}_2} \|\eta^1\|_0^2 + 5 \frac{\bar{C}_2 \bar{C}_1 \bar{B}_1 - \bar{C}_1^2 \bar{B}_2}{\bar{B}_1} \|\eta^2\|_0^2 \right] / (-\bar{B}_1 \bar{B}_2) \\
&= \frac{5}{2} M_1 \|\theta^0\|_0^2 + \frac{5}{2} M_2 [\Gamma(1 - \kappa)]^2 T^{2\kappa} \max_{i=1,2} \|R_\tau^i\|_0^2 + \frac{5}{2} M_1 \|\eta^0\|_0^2 + N_1 \|\eta^1\|_0^2 + N_2 \|\eta^2\|_0^2 \\
&\leq C(\tau^{3-\kappa} + N^{-q})^2,
\end{aligned}$$

where M_1, M_2 are defined in (3.5), and

$$N_1 = \frac{5(2 - \kappa)}{(1 - \kappa)(\kappa + 2)}, N_2 = \frac{5(2 - \kappa)}{16(1 - \kappa)^2}. \tag{3.22}$$

Based on (2.3), we have

$$\begin{aligned}
\|z_N^1 - z(\mathbf{x}, t_1)\|_2 &\leq \|\theta^1\|_2 + \|\eta^1\|_2 \leq \|\theta^1\|_2 + \|\eta^1\|_2 \\
&\leq C(\tau^{3-\kappa} + N^{-q}) + CN^{2-q} \leq C(\tau^{3-\kappa} + N^{2-q}).
\end{aligned}$$

Similarly, according to (3.20),

$$\|\theta^2\|_0^2 + \kappa_0 \beta_0^{-1} \|\Delta \theta^2\|_0^2 < \|\theta^2\|_0^2 + \frac{2\kappa_0}{\bar{C}_2} \|\Delta \theta^2\|_0^2$$

$$\begin{aligned}
&\leq 5 \frac{\bar{A}_2^2 \bar{B}_1 \bar{C}_1 - \bar{A}_1^2 \bar{B}_2 \bar{C}_2}{\bar{B}_1 \bar{C}_2^2 \bar{C}_1} \|\theta^0\|_0^2 + \left(\frac{5\kappa_0^2}{\bar{C}_2^2} - \frac{5\kappa_0^2 \bar{B}_2}{\bar{C}_2 \bar{B}_1 \bar{C}_1} \right)_{i=1,2} \max \|R_\tau^i\|_0^2 \\
&\quad + \left[5 \frac{\bar{A}_2^2 \bar{B}_1 \bar{C}_1 - \bar{A}_1^2 \bar{B}_2 \bar{C}_2}{\bar{B}_1 \bar{C}_2} \|\eta^0\|_0^2 + 5 \frac{\bar{B}_2^2 \bar{C}_1 - \bar{B}_2 \bar{B}_1 \bar{C}_2}{\bar{C}_2} \|\eta^1\|_0^2 + 5 \frac{\bar{C}_2 \bar{C}_1 \bar{B}_1 - \bar{C}_1^2 \bar{B}_2}{\bar{B}_1} \|\eta^2\|_0^2 \right] / (\bar{C}_1 \bar{C}_2) \\
&= \frac{5}{2} M_3 \|\theta^0\|_0^2 + \frac{5}{2} M_4 [\Gamma(1 - \kappa)]^2 T^{2\kappa} \max_{i=1,2} \|R_\tau^i\|_0^2 + \frac{5}{2} M_3 \|\eta^0\|_0^2 + N_3 \|\eta^1\|_0^2 + N_1 \|\eta^2\|_0^2 \\
&\leq C(\tau^{3-\kappa} + N^{-q})^2,
\end{aligned}$$

where M_3, M_4 are defined in (3.5), N_1 is defined in (3.22), and $N_3 = \frac{5(32 - 16\kappa)}{(\kappa + 2)^2}$. So we get

$$\begin{aligned}
\|z_N^2 - z(\mathbf{x}, t_2)\|_2 &\leq \|\theta^2\|_2 + \|\eta^2\|_2 \leq \|\theta^2\|_2 + \|\eta^2\|_2 \\
&\leq C(\tau^{3-\kappa} + N^{-q}) + CN^{2-q} \leq C(\tau^{3-\kappa} + N^{2-q}).
\end{aligned}$$

For $m \geq 3$, we obtain

$$\begin{aligned}
&(z(\mathbf{x}, t_m), v_N) + \kappa_0 \beta_0^{-1} (\Delta \mathbb{K}_{2,N}^0 z(\mathbf{x}, t_m), \Delta v_N) \\
&= \sum_{i=1}^m D_{m-i}^m (z(\mathbf{x}, t_{m-i}), v_N) + \kappa_0 \beta_0^{-1} (f^m, v_N) - \kappa_0 \beta_0^{-1} (R_\tau^m, v_N), \quad v_N \in Y_N.
\end{aligned} \tag{3.23}$$

By subtracting (2.5) from (3.23), we have

$$(\theta^m + \eta^m, v_N) + \kappa_0 \beta_0^{-1} (\Delta \theta^m, \Delta v_N) = \sum_{i=1}^m D_{m-i}^m (\theta^{m-i} + \eta^{m-i}, v_N) + \kappa_0 \beta_0^{-1} (R_\tau^m, v_N), \quad \forall v_N \in Y_N. \tag{3.24}$$

According to Lemma 2.1 and (3.24), it can be easily obtained that

$$\begin{aligned}
&(\theta^m, v_N) + \kappa_0 \beta_0^{-1} (\Delta \theta^m, \Delta v_N) \\
&= \sum_{i=1}^m D_{m-i}^m (\theta^{m-i}, v_N) - \left[(\eta^m, v_N) - \sum_{i=1}^m D_{m-i}^m (\eta^{m-i}, v_N) - \kappa_0 \beta_0^{-1} (R_\tau^m, v_N) \right] \\
&= \sum_{i=1}^m D_{m-i}^m (\theta^{m-i}, v_N) - (\mathbb{K}_{2,N}^0 z(\mathbf{x}, t_m) - z(\mathbf{x}, t_m), v_N) \\
&\quad + \sum_{i=1}^m D_{m-i}^m (\mathbb{K}_{2,N}^0 z(\mathbf{x}, t_{m-i}) - z(\mathbf{x}, t_{m-i}), v_N) + \kappa_0 \beta_0^{-1} (R_\tau^m, v_N) \\
&= \sum_{i=1}^m D_{m-i}^m (\theta^{m-i}, v_N) + (I - \mathbb{K}_{2,N}^0) (z(\mathbf{x}, t_m), v_N) \\
&\quad - (I - \mathbb{K}_{2,N}^0) \sum_{i=1}^m D_{m-i}^m (z(\mathbf{x}, t_{m-i}), v_N) + \kappa_0 \beta_0^{-1} (R_\tau^m, v_N) \\
&= \sum_{i=1}^m D_{m-i}^m (\theta^{m-i}, v_N) + (I - \mathbb{K}_{2,N}^0) (z(\mathbf{x}, t_m) - \sum_{i=1}^m D_{m-i}^m z(\mathbf{x}, t_{m-i}), v_N) + \kappa_0 \beta_0^{-1} (R_\tau^m, v_N) \\
&= \sum_{i=1}^m D_{m-i}^m (\theta^{m-i}, v_N) + (I - \mathbb{K}_{2,N}^0) (\kappa_0 \beta_0^{-1} (0 D_t^\kappa z(\mathbf{x}, t_m) - R_\tau^m, v_N)) + \kappa_0 \beta_0^{-1} (R_\tau^m, v_N)
\end{aligned}$$

$$\begin{aligned}
&= \sum_{i=1}^m D_{m-i}^m(\theta^{m-i}, v_N) + \kappa_0 \beta_0^{-1} ((I - \mathbb{K}_{2,N}^0) ({}_0 D_t^\kappa z(\mathbf{x}, t_m) - R_\tau^m) + R_\tau^m, v_N) \\
&= \sum_{i=1}^m D_{m-i}^m(\theta^{m-i}, v_N) + \kappa_0 \beta_0^{-1} (\zeta_N^m z, v_N), \quad \forall v_N \in Y_N,
\end{aligned} \tag{3.25}$$

where $\zeta_N^m z = (I - \mathbb{K}_{2,N}^0) ({}_0 D_t^\kappa z(\mathbf{x}, t_m) - R_\tau^m) + R_\tau^m$, I is the identity operator, and R_τ^m is defined by (2.2).

Applying the triangle inequality yields

$$\|\zeta_N^m z\|_0 \leq \|(I - \mathbb{K}_{2,N}^0) {}_0 D_t^\kappa z(\mathbf{x}, t_m)\|_0 + \|(I - \mathbb{K}_{2,N}^0) R_\tau^m\|_0 + \|R_\tau^m\|_0.$$

It can be obtained from Lemma 2.1 that

$$\|R_\tau^m\|_0 \leq C\tau^{3-\kappa},$$

and according to Lemma 3.3, it can be seen that

$$\|(I - \mathbb{K}_{2,N}^0) {}_0 D_t^\kappa z(\mathbf{x}, t_m)\|_0 \leq CN^{-q}.$$

Combining Lemmas 2.1 and 3.3, we have

$$\|(I - \mathbb{K}_{2,N}^0) R_\tau^m\|_0 \leq CN^{-q} \tau^{3-\kappa}.$$

Thus, we have

$$\|\zeta_N^m z\|_0 \leq C(\tau^{3-\kappa} + N^{-q} + \tau^{3-\kappa} N^{-q}). \tag{3.26}$$

Let $\bar{\theta}^i = \theta^i - \rho \theta^{i-1}$, $i = 2, \dots, K$, and it is observed that (3.25) can be rewritten in the following form:

$$\begin{aligned}
&(\bar{\theta}^m, v_N) + \kappa_0 \beta_0^{-1} (\Delta \theta^m, \Delta v_N) \\
&= \rho(\bar{\theta}^{m-1}, v_N) + \sum_{i=2}^{m-1} \bar{D}_{m-i}^m(\bar{\theta}^{m-i}, v_N) + \bar{D}_0^m(\bar{\theta}^0, v_N) + \kappa_0 \beta_0^{-1} (\zeta_N^m z, v_N),
\end{aligned}$$

where \bar{D}_j^m is defined in (3.1). The similar technique used in Theorem 3.1 enables us to obtain

$$\begin{aligned}
\|\theta^m\|_2^2 &= \|\theta^m\|_0^2 + \kappa_0 \beta_0^{-1} \|\Delta \theta^m\|_0^2 \\
&\leq H_1 \|\theta^0\|_0^2 + H_2 C_f [\Gamma(1 - \kappa)]^2 T^{2\kappa} \max_{1 \leq i \leq K} \|\zeta_N^i z\|_0^2 \\
&\leq C(\tau^{3-\kappa} + N^{-q} + \tau^{3-\kappa} N^{-q})^2.
\end{aligned}$$

Based on the above estimation and (2.3), we have

$$\begin{aligned}
\|z_N^m - z(\mathbf{x}, t_m)\|_2 &\leq \|\theta^m\|_2 + \|\eta^m\|_2 \leq \|\theta^m\|_2 + \|\eta^m\|_2 \\
&\leq C(\tau^{3-\kappa} + N^{-q} + \tau^{3-\kappa} N^{-q}) + CN^{2-q} \leq C(\tau^{3-\kappa} + N^{2-q}),
\end{aligned}$$

where C is a positive constant and independent of τ and N .

The proof is complete. \square

4. Numerical validation

4.1. Algorithm implementation

Before providing the calculation examples for verification, we briefly described the algorithm process with space dimension $d = 1$ for completeness. According to [29], we select the basis function as:

$$\phi_i(x) = \frac{1}{\sqrt{2(2i+3)^2(2i+5)}} \left[L_i(x) - \frac{2(2i+5)}{2i+7} L_{i+2}(x) + \frac{2i+3}{2i+7} L_{i+4}(x) \right], \quad i = 0, 1, \dots, N-4.$$

This satisfies $\phi(\pm 1) = \frac{\partial \phi}{\partial n}(\pm 1) = 0$. We choose an appropriate function space below:

$$Y_N = \{\phi_0(x), \phi_1(x), \dots, \phi_{N-4}(x)\}.$$

The function z_N^m is presented as

$$z_N^m = \sum_{j=0}^{N-4} z_j^m \phi_j(x).$$

We select $v_N = \phi_i(x)$ in scheme (2.5) and rewrite it for $m = 1, 2$ as follows:

$$\begin{aligned} \sum_{j=0}^{N-4} \left\{ \bar{B}_1(\phi_j, \phi_i) z_j^1 + \kappa_0(\Delta \phi_j, \Delta \phi_i) z_j^1 + \bar{C}_1(\phi_j, \phi_i) z_j^2 \right\} &= H_j^1, \\ \sum_{j=0}^{N-4} \left\{ \bar{B}_2(\phi_j, \phi_i) z_j^1 + \kappa_0(\Delta \phi_j, \Delta \phi_i) z_j^2 + \bar{C}_2(\phi_j, \phi_i) z_j^2 \right\} &= H_j^2, \end{aligned}$$

where the expressions for H_j^1 and H_j^2 are as follows:

$$\begin{aligned} H_j^1 &= \kappa_0(f^1, \phi_i) - \sum_{j=0}^{N-4} \bar{A}_1(\phi_j, \phi_i) z_j^0, \\ H_j^2 &= \kappa_0(f^2, \phi_i) - \sum_{j=0}^{N-4} \bar{A}_2(\phi_j, \phi_i) z_j^0. \end{aligned}$$

Let us denote

$$\begin{aligned} A &= \left[(\phi_j, \phi_i) \right]_{i,j=0}^{N-4}, & B &= \left[(\Delta \phi_j, \Delta \phi_i) \right]_{i,j=0}^{N-4}, \\ \mathbf{z}^m &= (z_0^m, z_1^m, \dots, z_{N-4}^m), & \mathbf{H}^m &= (H_0^m, H_1^m, \dots, H_{N-4}^m). \end{aligned}$$

We can obtain a matrix form:

$$\begin{pmatrix} \bar{B}_1 A + \kappa_0 B & \bar{C}_1 A \\ \bar{B}_2 A & \bar{C}_2 A + \kappa_0 B \end{pmatrix} \begin{pmatrix} (\mathbf{z}^1)^\top \\ (\mathbf{z}^2)^\top \end{pmatrix} = \begin{pmatrix} ((\mathbf{H}^1)^\top) \\ ((\mathbf{H}^2)^\top) \end{pmatrix}. \quad (4.1)$$

Solving (4.1), we obtain \mathbf{z}^1 and \mathbf{z}^2 .

Based on (2.5) for $m \geq 3$, we have

$$(A + \kappa_0 \beta_0^{-1} B) \mathbf{z}^m = \kappa_0 \beta_0^{-1} \mathbf{f}^m + A \sum_{i=1}^m D_{m-i}^m \mathbf{z}^{m-i}, \quad (4.2)$$

where

$$\mathbf{f}^m = (\bar{f}_0^m, \bar{f}_1^m, \dots, \bar{f}_{N-4}^m), \bar{f}_j^m = (f^m, \phi_i).$$

We solve (4.2) and get \mathbf{z}^m for $m \geq 3$.

4.2. Numerical results

In this part, we will use three examples to verify the accuracy of the theory, which proves the error estimation of the time step τ and the spatial polynomial N of the improved numerical scheme in solving fourth-order TFPDEs. Define

$$e_N(\tau) = \max_{1 \leq m \leq K} \|z(\mathbf{x}, t_m) - z_N^m\|_0,$$

and the convergence order in time is as follows:

$$\text{Order} = \log_2 \left(\frac{e_N(2\tau)}{e_N(\tau)} \right),$$

when N is sufficiently large.

Example 4.1. We choose

$$z(\mathbf{x}, t) = t^4 \sin^2 \pi x_1$$

as the smooth exact solution of (1.1), where $d = 1, \Omega = (-1, 1)$. It is easy obtained that $f(\mathbf{x}, t)$ is as follows:

$$f(\mathbf{x}, t) = \frac{\Gamma(5)}{\Gamma(5 - \kappa)} t^{4-\kappa} \sin^2 \pi x_1 + (8\pi^4 \sin^2 \pi x_1 - 8\pi^4 \cos^2 \pi x_1) t^4.$$

First, we check the temporal convergence order by choosing a sufficiently large spatial polynomial N , where the error caused by spatial approximation can be ignored.

In order to test the temporal order of accuracy, we choose $K = 2^m, m = 5, \dots, 9$, with $N = 80$ for different κ in Table 1. The convergence orders tend to 2.3, 2.5, 2.7, for $\kappa = 0.7, 0.5, 0.3$. It can be clearly observed that the temporal accuracy given by the scheme in terms of time is $(3 - \kappa)$, which is consistent with the result of Theorem 3.2.

Table 1. The errors and temporal convergence order with $\kappa = 0.3, 0.5$, and 0.7 .

τ	$\kappa = 0.3$	Order	$\kappa = 0.5$	Order	$\kappa = 0.7$	Order
$\frac{1}{32}$	2.63224×10^{-6}	—	9.31583×10^{-6}	—	2.86133×10^{-5}	—
$\frac{1}{64}$	4.33805×10^{-7}	2.60117	1.72424×10^{-6}	2.43372	6.01858×10^{-6}	2.24919
$\frac{1}{128}$	6.98610×10^{-8}	2.63449	3.12908×10^{-7}	2.46215	1.24452×10^{-6}	2.27384
$\frac{1}{256}$	1.10996×10^{-8}	2.65399	5.61859×10^{-8}	2.47746	2.55136×10^{-7}	2.28625
$\frac{1}{512}$	1.74841×10^{-9}	2.66639	1.00287×10^{-8}	2.48607	5.20733×10^{-8}	2.29265

Second, we consider the spatial spectral accuracy, by using a sufficiently small time step so that the resulting error does not affect the spatial accuracy. A logarithmic scale is now used for the error-axis. From Figure 1, we choose $N = 11, 13, \dots, 27$ and $K = 2^{12}$. For $\kappa = 0.3, 0.5, 0.7$, the errors decay exponentially with the increase of the approximation order of the spatial polynomial, and are close to 10^{-11} .

Finally, it can be found from Figure 1 that the error variation has a linear relationship with the polynomial order N . This indicates that the improved numerical scheme achieves spectral accuracy convergence in space. It is consistent with the theoretical result of Theorem 3.2.

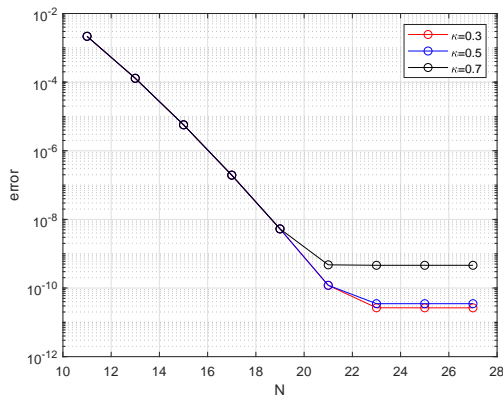


Figure 1. The error varies with the approximation order N of the spatial polynomial for $\kappa = 0.3, 0.5, 0.7$.

Similar to [30], in Tables 2 and 3, we selected the same parameters $K = 2^m, m = 5, \dots, 9$, with $N = 80$ as in Table 1 and discretized the time using the $L1$ and $L1 - L2$ schemes, respectively. When $\kappa = 0.3$ and $K = 2^9$, the error is 7.90177×10^{-7} in Table 2, while it is 1.74841×10^{-9} in Table 1. We find that the errors for different κ in Table 1 are smaller. The time convergence order is approximately $2 - \kappa$, while the order is $3 - \kappa$ in our Table 1. From the results of Table 3, we find that the $L1 - L2$ scheme convergence order is close to $3 - \kappa$ for large κ and τ . For small κ and τ , we find that the error is small but the convergence order is not close to $3 - \kappa$. That is to say, the impact of the first-step $L1$ scheme is more evident, which is easy to see from the last line in Table 3. It is easy to see that the errors of Table 1 are smaller than Table 3 for different κ . Therefore, the present $L2$ scheme has more significant advantages in terms of convergence order and absolute error than the $L1 - L2$ scheme.

Table 2. The errors and temporal convergence order with $\kappa = 0.3, 0.5$, and 0.7 in the $L1$ scheme.

τ	$\kappa = 0.3$	Order	$\kappa = 0.5$	Order	$\kappa = 0.7$	Order
$\frac{1}{32}$	7.43911×10^{-5}	—	2.55286×10^{-4}	—	7.50699×10^{-4}	—
$\frac{1}{64}$	2.43228×10^{-5}	1.61282	9.34308×10^{-5}	1.45015	3.11115×10^{-4}	1.27078
$\frac{1}{128}$	7.83541×10^{-6}	1.63423	3.37997×10^{-5}	1.46689	1.27850×10^{-4}	1.28300
$\frac{1}{256}$	2.49777×10^{-6}	1.64937	1.21369×10^{-5}	1.47761	5.22842×10^{-5}	1.29000
$\frac{1}{512}$	7.90177×10^{-7}	1.66039	4.33691×10^{-6}	1.48466	2.13215×10^{-5}	1.29406

Table 3. The errors and temporal convergence order with $\kappa = 0.3, 0.5$, and 0.7 in the $L1 - L2$ scheme.

τ	$\kappa = 0.3$	Order	$\kappa = 0.5$	Order	$\kappa = 0.7$	Order
$\frac{1}{32}$	2.72560×10^{-6}	—	9.63809×10^{-6}	—	2.95938×10^{-5}	—
$\frac{1}{64}$	4.41289×10^{-7}	2.62678	1.75302×10^{-6}	2.45890	6.11839×10^{-6}	2.27407
$\frac{1}{128}$	7.10401×10^{-8}	2.63502	3.15601×10^{-7}	2.47367	1.25470×10^{-6}	2.28581
$\frac{1}{256}$	1.44507×10^{-8}	2.29749	5.71581×10^{-8}	2.46507	2.56332×10^{-7}	2.29126
$\frac{1}{512}$	9.36375×10^{-7}	0.62598	1.36232×10^{-8}	2.06890	5.29827×10^{-8}	2.27442

Example 4.2. In this example, we consider the non-smooth exact solution of problem (1.1) as $z(\mathbf{x}, t) = t^\kappa \sin^2 \pi x_1$ for $d = 1, \Omega = (-1, 1)$. Through calculation, we can obtain the right-hand term $f(\mathbf{x}, t)$ as follows:

$$f(\mathbf{x}, t) = \Gamma(1 + \kappa) \sin^2 \pi x_1 + (8\pi^4 \sin^2 \pi x_1 - 8\pi^4 \cos^2 \pi x_1)t^\kappa.$$

We can see that this exact solution does not meet the conditions of Theorem 3.2. Similar to [31], we need to use the graded mesh $t_m = (\frac{m}{K})^r, m = 1, \dots, K$, to increase the order of temporal convergence. We have adopted two different sets of r parameters. When $T = 1$, the errors and convergence orders of different κ and r in the time direction are shown in Tables 4 and 5.

First, when $r = 1$, it is a uniform mesh. In Table 4, for $K = 32, 64, 128, 256, 512$ and $N = 80$, due to the low regularity of the exact solution, the convergence order is also low for $\kappa = 0.3, 0.5$, and 0.7 . Therefore, we adopt graded mesh to improve the convergence order.

Table 4. The maximum errors and temporal convergence orders with $T = 1, \tau = \frac{1}{K}, N = 80$, and $r = 1$.

τ	$\kappa = 0.3$	Order	$\kappa = 0.5$	Order	$\kappa = 0.7$	Order
$\frac{1}{32}$	3.76959×10^{-1}	—	2.16506×10^{-1}	—	1.24350×10^{-1}	—
$\frac{1}{64}$	3.06186×10^{-1}	0.30000	1.53093×10^{-1}	0.49999	7.65466×10^{-2}	0.69999
$\frac{1}{128}$	2.48700×10^{-1}	0.30000	1.08253×10^{-1}	0.50000	4.71199×10^{-2}	0.70000
$\frac{1}{256}$	2.02008×10^{-1}	0.30000	7.65466×10^{-2}	0.49999	2.90057×10^{-2}	0.70000
$\frac{1}{512}$	1.64081×10^{-1}	0.29999	5.41266×10^{-2}	0.50000	1.78551×10^{-2}	0.69999

Second, in order to reach the theoretical order, we choose $r = (3 - \kappa)/\kappa$. The error and time convergence order of the obtained numerical solutions are listed in Table 5 for different κ . It is easy for us to notice that the temporal convergence orders gradually decrease with the increase of the value of κ , which is consistent with our theoretical analysis.

Table 5. The maximum errors and temporal convergence orders with $T = 1$, $\tau = \frac{1}{K}$, $N = 80$, and $r = (3 - \kappa)/\kappa$.

τ	$\kappa = 0.3$	Order	$\kappa = 0.5$	Order	$\kappa = 0.7$	Order
$\frac{1}{32}$	1.51160×10^{-3}	—	1.65086×10^{-3}	—	5.59258×10^{-4}	—
$\frac{1}{64}$	3.48304×10^{-4}	2.11765	3.73259×10^{-4}	2.14497	1.50613×10^{-4}	1.89267
$\frac{1}{128}$	7.00722×10^{-5}	2.31343	8.06936×10^{-5}	2.20965	3.85068×10^{-5}	1.96766
$\frac{1}{256}$	1.19702×10^{-5}	2.54939	1.51649×10^{-5}	2.41172	9.01072×10^{-6}	2.09540
$\frac{1}{512}$	1.91404×10^{-6}	2.64475	2.71390×10^{-6}	2.48229	1.94391×10^{-6}	2.21268

Finally, on the graded grid $r = (3 - \kappa)/\kappa$, we fix $N = 9, 11, \dots, 25$, $T = 1$, $K = 2^{12}$. These values are sufficient to make the temporal errors negligible compared with the spatial error for $\kappa = 0.3, 0.5, 0.7$ in Figure 2. As expected, the error variation basically has a linear relationship with the approximation order of the spatial polynomial and eventually tends to stabilize. We verify that the new numerical algorithm has high accuracy even when the exact solution is a low smoothness.

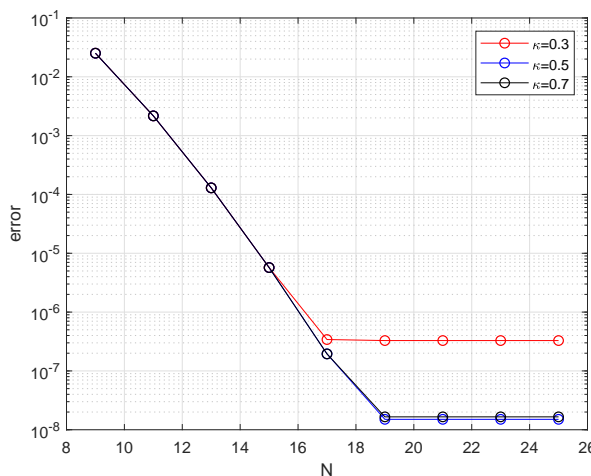


Figure 2. The error varies with N in Example 4.2 with $r = (3 - \kappa)/\kappa$ for $\kappa = 0.3, 0.5, 0.7$.

Example 4.3. We consider the following equations:

$$\begin{cases} {}_0D_t^\kappa z(\mathbf{x}, t) + \Delta^2 z(\mathbf{x}, t) = f(\mathbf{x}, t) + z(\mathbf{x}, t) - z^3(\mathbf{x}, t), & \text{in } \Omega, \\ z(\mathbf{x}, t) = \frac{\partial z(\mathbf{x}, t)}{\partial n} = 0, & \text{on } \partial\Omega, \\ z(\mathbf{x}, 0) = 0, & \text{in } \Omega. \end{cases}$$

Case 1. The space is one-dimensional. Given the exact solution $z(\mathbf{x}, t) = t^4 \sin^2 \pi x_1$, $\Omega = (-1, 1)$. The source term $f(\mathbf{x}, t)$ can be directly obtained through calculations:

$$f(\mathbf{x}, t) = \frac{\Gamma(5)}{\Gamma(5 - \kappa)} t^{4 - \kappa} \sin^2 \pi x_1 + (8\pi^4 \sin^2 \pi x_1 - 8\pi^4 \cos^2 \pi x_1) t^4 + t^{12} \sin^6 \pi x_1 - t^4 \sin^2 \pi x_1.$$

We set $T = 1$, the step size $\tau = \frac{1}{K}$, and $K = 2^m$.

Table 6 gives the maximum errors and temporal convergence order of the proposed scheme for different κ . We choose $m = 4, \dots, 8$ and $N = 80$. The results show that the temporal convergence order $(3 - \kappa)$ is highly consistent with the theoretical expectation.

Table 6. The errors and temporal convergence orders for Example 4.3 with $\kappa = 0.3, 0.5$, and 0.7 .

τ	$\kappa = 0.3$	Order	$\kappa = 0.5$	Order	$\kappa = 0.7$	Order
$\frac{1}{16}$	1.64970×10^{-5}	—	5.21424×10^{-5}	—	1.41468×10^{-4}	—
$\frac{1}{32}$	2.73061×10^{-6}	2.59491	9.66438×10^{-6}	2.43171	2.97138×10^{-5}	2.25127
$\frac{1}{64}$	4.42106×10^{-7}	2.62676	1.75784×10^{-6}	2.45887	6.14340×10^{-6}	2.27402
$\frac{1}{128}$	7.11698×10^{-8}	2.63505	3.16471×10^{-7}	2.47366	1.25984×10^{-6}	2.28580
$\frac{1}{256}$	1.44667×10^{-8}	2.69853	5.73118×10^{-8}	2.46517	2.57382×10^{-7}	2.29126

In Figure 3, we plot the obtained errors for $N = 11, \dots, 27$ and $K = 2^{10}$ based on different values of κ . The variation of the error is also linearly related to the approximation order of the spatial polynomial and eventually tends to stabilize. From Table 6 and Figure 3, it can be see that the method studied in this paper can numerically solve nonlinear spatial fourth-order partial differential equations with time fractional derivative.

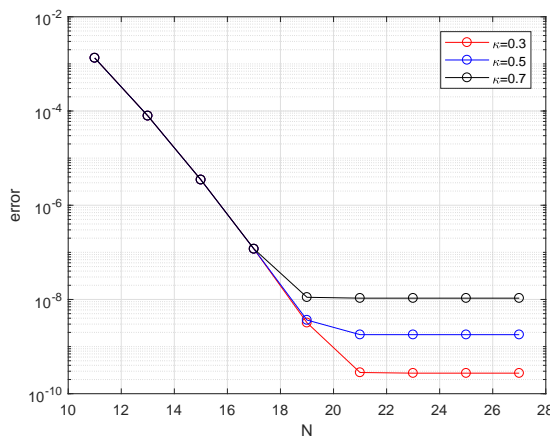


Figure 3. The error varies with N for Example 4.3 for $\kappa = 0.3, 0.5, 0.7$.

Case 2. The space is two-dimensional. The exact solution of the equation is $z(\mathbf{x}, t) = t^4 \sin^2 2\pi x_1 \sin^2 2\pi x_2$, $\Omega = (-1, 1) \times (-1, 1)$, and the corresponding function $f(\mathbf{x}, t)$ is

$$f(\mathbf{x}, t) = \frac{\Gamma(5)}{\Gamma(5 - \kappa)} t^{4-\kappa} \sin^2 2\pi x_1 \sin^2 2\pi x_2 + 128\pi^4 t^4 (\cos 4\pi x_1 \cos 4\pi x_2 - \cos 4\pi x_1 \sin^2 2\pi x_2 - \cos 4\pi x_2 \sin^2 2\pi x_1) + t^{12} \sin^6 2\pi x_1 \sin^6 2\pi x_2 - t^4 \sin^2 2\pi x_1 \sin^2 2\pi x_2.$$

Fix $m = 2, \dots, 6$ and $N = 120$. Table 7 shows the errors and temporal convergence orders of the method for $\kappa = 0.4, 0.6, 0.8$ with different τ . The results in this table confirm that the scheme has $(3 - \kappa)$ temporal accuracy.

Table 7. The errors and temporal convergence orders for Example 4.3 with $\kappa = 0.4, 0.6$, and 0.8 .

τ	$\kappa = 0.4$	Order	$\kappa = 0.6$	Order	$\kappa = 0.8$	Order
$\frac{1}{4}$	1.96963×10^{-4}	—	5.30046×10^{-4}	—	1.04878×10^{-3}	—
$\frac{1}{8}$	3.86943×10^{-5}	2.34773	9.92428×10^{-5}	2.41708	2.27435×10^{-4}	2.20519
$\frac{1}{16}$	7.01935×10^{-6}	2.46271	2.02014×10^{-5}	2.29651	5.24735×10^{-5}	2.11582
$\frac{1}{32}$	1.22720×10^{-6}	2.51597	3.98027×10^{-6}	2.34352	1.17586×10^{-5}	2.15784
$\frac{1}{64}$	2.13088×10^{-7}	2.52585	7.76810×10^{-7}	2.35723	2.59946×10^{-6}	2.17744

To test the accuracy in space, we present the plot of the error at different N for $\kappa = 0.4, 0.6, 0.8$ and $K = 2^{10}$. As we can see, the results of Figure 4 confirm the accuracy of the method in space.

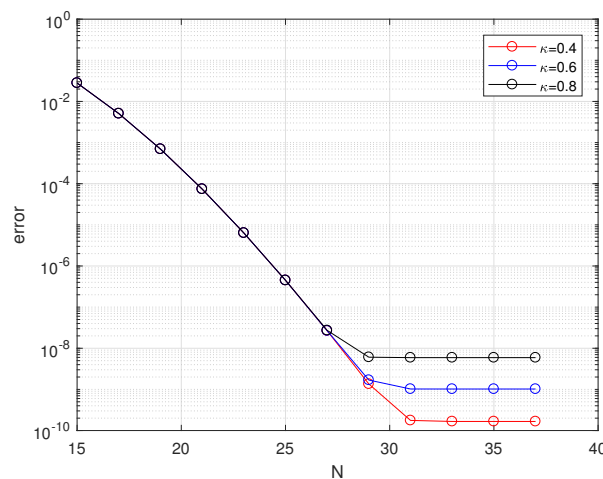


Figure 4. The error varies with N for Example 4.3 for $\kappa = 0.4, 0.6, 0.8$.

5. Concluding remarks

An improved scheme for the fourth-order TFPDE is established by using the temporal uniform convergence order $L2$ scheme and spatial Galerkin spectral method. Based on the properties of the inverse Laplace operator, the stability and convergence of the present scheme are proved. This novel stability analysis method has significant reference value for the theoretical analysis of spatial high-order derivative equations. Through experiments, we have verified that this improved numerical scheme can be used to solve high-dimensional nonlinear fourth-order TFPDEs. In the future, we will focus on adapting the present scheme to solve fourth-order TFPDE optimal control problems using the ideas in [32]. Considering the high computational efficiency of the present high-order uniform temporal numerical scheme, we will establish a fast algorithm to solve fourth-order TFPDEs based on the sum-of-exponential method using ideas from [26]. The research on efficient numerical algorithms for optimal control problems of fractional-order integral differential equations is also a hot topic. Based on the methods of three-layer FDM [33], alternating direction implicit difference scheme [34, 35], superconvergence analysis [36], shifted Chebyshev-Galerkin operational matrix methods [37], Hexic shifted Chebyshev polynomials [38], spectral collocation [39], Lucas polynomial approximation [40],

spectral Tau method [41], Cutting-edge spectral [42] and the algorithm proposed in this paper, we will study high-precision numerical algorithms for optimal control problems of fractional-order integral differential equations.

Author contributions

Hanmei Jian: Formal analysis, investigation, resources, writing – original draft, validation, and data curation; Junying Cao: Formal analysis, investigation, writing – review and editing; Ziqiang Wang: Project administration, methodology, data curation, validation, and formal funding acquisition. All authors have read and approved the final version of the manuscript for publication.

Use of Generative-AI tools declaration

The authors declare that they have not used Artificial Intelligence (AI) tools in the creation of this article.

Acknowledgments

The work was supported by the National Natural Science Foundation of China (Grant Nos. 12361083, 12461077, and 11961009), Science Research Fund Support Project of Guizhou Minzu University (Grant No. GZMUZK[2023]CXTD05), Foundation of Guizhou Science and Technology Department (Grant No. QHKJC-ZK[2024]YB497), Natural Science Foundation of the Department of Education of Guizhou Province (Grant No. QJJ2023012), and High-Level Innovative Talent Project of Guizhou Province (Grant No. QKHPTRC-GCC2023027).

Conflict of interest

The authors declare that they have no competing interests.

References

1. J. B. Greer, A. L. Bertozzi, G. Sapiro, Fourth order partial differential equations on general geometries, *J. Comput. Phys.*, **216** (2006), 216–246. <https://doi.org/10.1016/j.jcp.2005.11.031>
2. X. Yang, W. Wang, Z. Zhou, H. Zhang, An efficient compact difference method for the fourth-order nonlocal subdiffusion problem, *Taiwanese J. Math.*, **29** (2025), 35–66. <https://doi.org/10.11650/tjm/240906>
3. H. Tariq, G. Akram, Quintic spline technique for time fractional fourth-order partial differential equation, *Numer. Methods Partial Differential Equations*, **33** (2017), 445–466. <https://doi.org/10.1002/num.22088>
4. M. Fei, C. Huang, Galerkin-Legendre spectral method for the distributed-order time fractional fourth-order partial differential equation, *Int. J. Comput. Math.*, **97** (2020), 1183–1196. <https://doi.org/10.1080/00207160.2019.1608968>

5. Y. Liu, Z. Fang, H. Li, S. He, A mixed finite element method for a time-fractional fourth-order partial differential equation, *Appl. Math. Comput.*, **243** (2014), 703–717. <https://doi.org/10.1016/j.amc.2014.06.023>
6. M. Dehghan, M. Safarpoor, Application of the dual reciprocity boundary integral equation approach to solve fourth-order time-fractional partial differential equations, *Int. J. Comput. Math.*, **95** (2018), 2066–2081. <https://doi.org/10.1080/00207160.2017.1365141>
7. Y. Chen, J. Zhou, Error estimates of spectral Legendre-Galerkin methods for the fourth-order equation in one dimension, *Appl. Math. Comput.*, **268** (2015), 1217–1226. <https://doi.org/10.1016/j.amc.2015.06.082>
8. D. Xu, W. Qiu, J. Guo, A compact finite difference scheme for the fourth-order time-fractional integro-differential equation with a weakly singular kernel, *Numer. Methods Partial Differential Equations*, **36** (2020), 439–458. <https://doi.org/10.1002/num.22436>
9. M. Cui, Compact difference scheme for time-fractional fourth-order equation with first Dirichlet boundary condition, *East Asian J. Appl. Math.*, **9** (2019), 45–66. <https://doi.org/10.4208/eajam.260318.220618>
10. P. Roul, V. M. K. P. Goura, A high order numerical method and its convergence for time-fractional fourth order partial differential equations, *Appl. Math. Comput.*, **366** (2020), 124727. <https://doi.org/10.1016/j.amc.2019.124727>
11. F. Fakhar-Izadi, Fully Petrov-Galerkin spectral method for the distributed-order time-fractional fourth-order partial differential equation, *Eng. Comput.*, **37** (2021), 2707–2716. <https://doi.org/10.1007/s00366-020-00968-2>
12. F. Fakhar-Izadi, Fully spectral-Galerkin method for the one- and two- dimensional fourth-order time-fractional partial integro-differential equations with a weakly singular kernel, *Numer. Methods Partial Differential Equations*, **38** (2022), 160–176. <https://doi.org/10.1002/num.22634>
13. M. Hagh, M. Ilati, M. Dehghan, A fourth-order compact difference method for the nonlinear time-fractional fourth-order reaction-diffusion equation, *Eng. Comput.*, **39** (2023), 1329–1340. <https://doi.org/10.1007/s00366-021-01524-2>
14. Y. Zhang, M. Feng, A mixed virtual element method for the time-fractional fourth-order subdiffusion equation, *Numer. Algor.*, **90** (2022), 1617–1637. <https://doi.org/10.1007/s11075-021-01244-0>
15. D. A. Koç, A numerical scheme for time-fractional fourth-order reaction-diffusion model, *J. Appl. Math. Comput. Mech.*, **22** (2023), 15–25. <https://doi.org/10.17512/jamcm.2023.2.02>
16. Z. Wang, Numerical analysis of local discontinuous Galerkin method for the time-fractional fourth-order equation with initial singularity, *Fractal Fract.*, **6** (2022), 206. <https://doi.org/10.3390/fractfract6040206>
17. Y. Wang, S. Yi, A compact difference-Galerkin spectral method of the fourth-order equation with a time-fractional derivative, *Fractal Fract.*, **9** (2025), 155. <https://doi.org/10.3390/fractfract9030155>

18. M. Abbaszadeh, M. Dehghan, Direct meshless local Petrov-Galerkin (DMLPG) method for time-fractional fourth-order reaction-diffusion problem on complex domains, *Comput. Math. Appl.*, **79** (2020), 876–888. <https://doi.org/10.1016/j.camwa.2019.08.001>

19. M. A. Abdelkawy, M. M. Babatin, A. M. Lopes, Highly accurate technique for solving distributed-order time-fractional-sub-diffusion equations of fourth order, *Comput. Appl. Math.*, **39** (2020), 65. <https://doi.org/10.1007/s40314-020-1070-7>

20. J. Zheng, J. An, Spectral Galerkin approximation and error analysis based on a mixed scheme for fourth-order problems in complex regions, *Numer. Methods Partial Differential Equations*, **41** (2025), e23154. <https://doi.org/10.1002/num.23154>

21. J. Zheng, J. An, A Legendre spectral-Galerkin method for fourth-order problems in cylindrical regions, *Numer. Methods Partial Differential Equations*, **40** (2024), e23071. <https://doi.org/10.1002/num.23071>

22. X. Yu, B. Guo, Spectral method for fourth-order problems on quadrilaterals, *J. Sci. Comput.*, **66** (2016), 477–503. <https://doi.org/10.1007/s10915-015-0031-6>

23. H. Fakhari, A. Mohebbi, Galerkin spectral and finite difference methods for the solution of fourth-order time fractional partial integro-differential equation with a weakly singular kernel, *J. Appl. Math. Comput.*, **70** (2024), 5063–5080. <https://doi.org/10.1007/s12190-024-02173-6>

24. Y. Du, Y. Liu, H. Li, Z. Fang, S. He, Local discontinuous Galerkin method for a nonlinear time-fractional fourth-order partial differential equation, *J. Comput. Phys.*, **344** (2017), 108–126. <https://doi.org/10.1016/j.jcp.2017.04.078>

25. S. S. Siddiqi, S. Arshed, Numerical solution of time-fractional fourth-order partial differential equations, *Inter. J. Comput. Math.*, **92** (2015), 1496–1518. <https://doi.org/10.1080/00207160.2014.948430>

26. H. Zhu, C. Xu, A fast high order method for the time-fractional diffusion equation, *SIAM J. Numer. Anal.*, **57** (2019), 2829–2849. <https://doi.org/10.1137/18M1231225>

27. F. Fakhar-Izadi, N. Shabgard, Time-space spectral Galerkin method for time-fractional fourth-order partial differential equations, *J. Appl. Math. Comput.*, **68** (2022), 4253–4272. <https://doi.org/10.1007/s12190-022-01707-0>

28. J. Cao, Z. Wang, Z. Wang, A uniform accuracy high-order finite difference and FEM for optimal problem governed by time-fractional diffusion equation, *Fractal Fract.*, **6** (2022), 475. <https://doi.org/10.3390/fractfract6090475>

29. J. Shen, Efficient spectral-Galerkin method I. Direct solvers of second- and fourth-order equations using Legendre polynomials, *SIAM J. Sci. Comput.*, **15** (1994), 1489–1505. <https://doi.org/10.1137/0915089>

30. Y. Lin, C. Xu, Finite difference/spectral approximations for the time-fractional diffusion equation, *J. Comput. Phys.*, **225** (2007), 1533–1552. <https://doi.org/10.1016/j.jcp.2007.02.001>

31. H. Qiao, A. Cheng, A fast high order method for time fractional diffusion equation with non-smooth data, *Discrete Contin. Dyn. Syst. Ser. B*, **27** (2022), 903–920. <https://doi.org/10.3934/dcdsb.2021073>

32. Z. Tao, B. Sun, Galerkin spectral method for a fourth-order optimal control problem with H^1 -norm state constraint, *Comput. Math. Appl.*, **97** (2021), 1–17. <https://doi.org/10.1016/j.camwa.2021.05.023>

33. J. Zhang, X. Yang, S. Wang, A three-layer FDM for the Neumann initial-boundary value problem of 2D Kuramoto-Tsuzuki complex equation with strong nonlinear effects, *Commun. Nonlinear Sci. Numer. Simul.*, **152** (2026), 109255. <https://doi.org/10.1016/j.cnsns.2025.109255>

34. Z. Zhang, X. Yang, S. Wang, The alternating direction implicit difference scheme and extrapolation method for a class of three dimensional hyperbolic equations with constant coefficients, *Electron. Res. Arch.*, **33** (2025), 3348–3377. <https://doi.org/10.3934/era.2025148>

35. J. Zhang, X. Yang, S. Wang, The ADI difference and extrapolation scheme for high-dimensional variable coefficient evolution equations, *Electron. Res. Arch.*, **33** (2025), 3305–3327. <https://doi.org/10.3934/era.2025146>

36. X. Yang, Z. Zhang, Superconvergence analysis of a robust orthogonal Gauss collocation method for 2D fourth-order subdiffusion equations, *J. Sci. Comput.*, **100** (2024), 62. <https://doi.org/10.1007/s10915-024-02616-z>

37. M. Abdelhakem, D. Abdelhamied, M. El-Kady, Y. H. Youssri, Two modified shifted Chebyshev-Galerkin operational matrix methods for even-order partial boundary value problems, *Bound. Value Probl.*, **2025** (2025), 34. <https://doi.org/10.1186/s13661-025-02021-x>

38. A. G. Atta, J. F. Soliman, E. W. Elsaeed, M. W. Elsaeed, Y. H. Youssri, Spectral collocation algorithm for the fractional Bratu equation via Hexic shifted Chebyshev polynomials, *Comput. Methods Differ. Equ.*, **13** (2025), 1102–1116. <https://doi.org/10.22034/cmde.2024.61045.2621>

39. Y. H. Youssri, S. M. Sayed, Efficient spectral collocation algorithm for pantograph integro-differential equations involving delay and weakly singular kernels, *J. Umm Al-Qura Univ. Appl. Sci.*, 2025. <https://doi.org/10.1007/s43994-025-00274-x>

40. Y. H. Youssri, A. G. Atta, A spectral Tau method based on Lucas polynomial approximation for solving the nonlinear fractional Riccati equation, *Comput. Methods Differ. Equ.*, 2025, In press. <https://doi.org/10.22034/cmde.2025.67681.3237>

41. S. G. Kamel, A. G. Atta, Y. H. Youssri, An explicit spectral Tau method with Delannoy polynomials for the time-fractional diffusion equation, *Open. J. Math. Anal.*, **9** (2025), 134–144. <https://doi.org/10.30538/psrp-oma2025.0169>

42. A. M. Abbas, Y. H. Youssri, M. El-Kady, M. Abdelhakem, Cutting-edge spectral solutions for differential and integral equations utilizing Legendre's derivatives, *Iran. J. Numer. Anal. Optim.*, **15** (2025), 1036–1074. <https://doi.org/10.22067/ijnao.2025.91804.1590>



AIMS Press

© 2025 the Author(s), licensee AIMS Press. This is an open access article distributed under the terms of the Creative Commons Attribution License (<http://creativecommons.org/licenses/by/4.0>)